



Daily burned area and carbon emissions from boreal fires in Alaska

S. Veraverbeke¹, B. M. Rogers², and J. T. Randerson¹

¹Department of Earth System Science, University of California, Irvine, California, USA

²Woods Hole Research Center, Falmouth, Massachusetts, USA

Correspondence to: S. Veraverbeke (sander.veraverbeke@uci.edu)

Received: 7 November 2014 – Published in Biogeosciences Discuss.: 18 December 2014

Revised: 4 April 2015 – Accepted: 7 May 2015 – Published: 10 June 2015

Abstract. Boreal fires burn into carbon-rich organic soils, thereby releasing large quantities of trace gases and aerosols that influence atmospheric composition and climate. To better understand the factors regulating boreal fire emissions, we developed a statistical model of carbon consumption by fire for Alaska with a spatial resolution of 450 m and a temporal resolution of 1 day. We used the model to estimate variability in carbon emissions between 2001 and 2012. Daily burned area was mapped using imagery from the Moderate Resolution Imaging Spectroradiometer combined with perimeters from the Alaska Large Fire Database. Carbon consumption was calibrated using available field measurements from black spruce forests in Alaska. We built two nonlinear multiplicative models to separately predict above- and belowground carbon consumption by fire in response to environmental variables including elevation, day of burning within the fire season, pre-fire tree cover and the differenced normalized burn ratio (dNBR). Higher belowground carbon consumption occurred later in the season and for mid-elevation forests. Topographic slope and aspect did not improve performance of the belowground carbon consumption model. Aboveground and belowground carbon consumption also increased as a function of tree cover and the dNBR, suggesting a causal link between the processes regulating these two components of carbon consumption. Between 2001 and 2012, the median carbon consumption was 2.54 kg C m^{-2} . Burning in land-cover types other than black spruce was considerable and was associated with lower levels of carbon consumption than for pure black spruce stands. Carbon consumption originated primarily from the belowground fraction (median = 2.32 kg C m^{-2} for all cover types and 2.67 kg C m^{-2} for pure black spruce stands). Total carbon emissions varied considerably from year to year, with the highest emissions occurring during 2004 (69 TgC), 2005 (46 TgC), 2009 (26 TgC),

and 2002 (17 TgC) and a mean of $15 \text{ Tg C year}^{-1}$ between 2001 and 2012. Mean uncertainty of carbon consumption for the domain, expressed as 1 standard deviation (SD), was 0.50 kg C m^{-2} . Uncertainties in the multiplicative regression model used to estimate belowground consumption in black spruce stands and the land-cover classification were primary contributors to uncertainty estimates. Our analysis highlights the importance of accounting for the spatial heterogeneity of fuels and combustion when extrapolating emissions in space and time, and the need for additional field campaigns to increase the density of observations as a function of tree cover and other environmental variables influencing consumption. The daily emissions time series from the Alaskan Fire Emissions Database (AKFED) presented here creates new opportunities to study environmental controls on daily fire dynamics, optimize boreal fire emissions in biogeochemical models, and quantify potential feedbacks from changing fire regimes.

1 Introduction

Fire is the most important landscape disturbance in the boreal forest (Chapin et al., 2000; Krawchuk et al., 2006). Increases in the extent and severity of burning in the last several decades have been reported for Alaska and Canada (Gillett et al., 2004; Kasischke and Turetsky, 2006; Kasischke et al., 2010; Turetsky et al., 2011). Fire regimes are expected to intensify (Amiro et al., 2009; Balshi et al., 2009; Yuan et al., 2012; de Groot et al., 2013) with the predicted accelerated warming for the boreal region during the remainder of the 21st century (Collins et al., 2013), although this may be mediated in part by changing vegetation cover (Krawchuk and Cumming, 2011; Mann et al., 2012; Kelly et al., 2013;

Héon et al., 2014). Boreal fires have both positive and negative climate feedbacks (Randerson et al., 2006; Bowman et al., 2009; Oris et al., 2014; Rogers et al., 2015). Cooling is primarily caused by increases in surface albedo from more exposed snow cover during spring in young stands (Jin et al., 2012; Rogers et al., 2013) and the influence of organic carbon aerosols on tropospheric radiation (Tosca et al., 2013). Emission of greenhouse gases, black carbon aerosols (Bowman et al., 2009), and the deposition of black carbon on snow and ice (Flanner et al., 2007) are the dominant warming feedbacks.

The magnitudes of these feedbacks are tightly linked with the severity of the disturbance (Beck et al., 2011a; Turetsky et al., 2011; Jin et al., 2012). Severity is often referred to in a general way describing the amount of environmental damage that fire causes to an ecosystem (Key and Benson, 2006). In the context of mostly stand-replacing fires in boreal North America, severity is expressed as the degree of consumption of belowground organic matter. Differences in ground layer burn depths control the amount of carbon combusted, and impact post-fire succession trajectories and consequent albedo feedbacks (Johnstone and Kasischke, 2005; Johnstone et al., 2010; Jin et al., 2012). Heterogeneity in fuels, fuel conditions, topography and fire weather can result in different post-fire effects over the landscape (Rogers et al., 2015). Resolving the spatial heterogeneity in severity using post-fire remote-sensing observations can improve emissions estimates (Michalek et al., 2000; Veraverbeke and Hook, 2013; Rogers et al., 2014) and more accurate carbon emissions estimates could lower the uncertainties in estimating the net climate feedback from boreal fires under the current and future climate (Oris et al., 2014).

Fire emissions are generally calculated as the product of burned area, fuel consumption and emission factors (Seiler and Crutzen, 1980). Fuel consumption represents the amount of biomass consumed by the fire, and gas-specific emission factors describe the amount of gas released per unit of biomass consumed by the fire. Examples of models building on this paradigm at continental or global scales include the Wildland Fire Emissions Information System (WFEIS, French et al., 2011, 2014) and the Global Fire Emissions Database version 3 (GFED3, van der Werf et al., 2010), updated with contributions of small fires (GFED3s, Randerson et al., 2012). Several similar approaches have been developed specifically for boreal forests (Kasischke et al., 1995; Amiro et al., 2001; Kajii et al., 2002; Kasischke and Bruhwiler, 2002; French et al., 2003; Soja et al., 2004; de Groot et al., 2007; Tan et al., 2007; Kasischke and Hoy, 2012). The quantification of fuel consumption in boreal emission models is often driven by empirical relationships between fire-weather variables and combustion completeness that vary by fuel type (Amiro et al., 2001; de Groot et al., 2007; Ottmar, 2014). A defining characteristic of fire emissions in the boreal forest is that mass of fuel consumed in the ground layer (comprised of moss, lichens, litter, and organic soils) is larger

than the consumption of aboveground biomass (McGuire et al., 2009; Boby et al., 2010; Kasischke and Hoy, 2012). Because of the seasonal thawing of the permafrost, the active layer becomes deeper and drier throughout the fire season and thus more prone to deeper burning (Lapina et al., 2008; Turetsky et al., 2011; Kasischke and Hoy, 2012). Based on this rationale, several authors have developed scenarios in which they assign ground fuel consumption values based on the seasonality of the burn (Kajii et al., 2002; Kasischke and Bruhwiler, 2002; Soja et al., 2004). The dryness of the forest floor depends both on the time within the season and local drainage conditions (Kane et al., 2007; Turetsky et al., 2011). Kasischke and Hoy (2012) incorporated this expert knowledge to derive emissions from a set of Alaskan fires by accounting for differential impacts of fire seasonality on several topographic classes.

Several studies have demonstrated relatively strong relationships between post-fire remote-sensing observations and ground layer consumption in boreal forest ecosystems (Hudak et al., 2007; Verbyla and Lord, 2008; Rogers et al., 2014). Identification of such relationships may provide opportunities to constrain pyrogenic carbon emission estimates in boreal forest ecosystems at regional to pan-boreal scales (Ottmar, 2014). Quantifying relationships between field data of carbon consumption and pre- and post-fire remote-sensing observations, in combination with other environmental variables, may minimize the number of assumptions required to extrapolate emissions in time and space. In addition, observed variability in relationships between field observations and environmental variables may allow for a data-driven approach for uncertainty quantification. Spectral changes after a fire have shown to be strongly related to field measurements of severity in a wide range of ecosystems (e.g., van Wagtenonk et al., 2004; Cocker et al., 2005; De Santis and Chuvieco, 2007; Veraverbeke and Hook, 2013), including the boreal forest (Epting et al., 2005; Allen and Sorbel, 2008; Hall et al., 2008; Soverel et al., 2010). Severity is often referred to as fire severity or burn severity (Lentile et al., 2006; Keeley, 2009) with the difference in definition between the two terms associated with the temporal dimension of fire effects. By definition, fire severity measures the immediate impact of the fire, whereas burn severity incorporates both the immediate fire impact and subsequent recovery effects (Lentile et al., 2006; French et al., 2008; Veraverbeke et al., 2010). In particular, the differenced normalized burn ratio (dNBR) has become accepted as a standard spectral index to assess severity (López García and Caselles, 1991; Key and Benson, 2006). dNBR is an index that combines near and short-wave infrared reflectance values obtained before and after a fire (Eidenshink et al., 2007). The spectral regions in dNBR are especially sensitive to the decrease of vegetation productivity and moisture content after the fire. Because of this, dNBR is a good indicator of aboveground biomass consumption, but may be less effective in estimating belowground consumption of boreal fires (French et al., 2008; Hoy

et al., 2008; Kasischke et al., 2008). Other studies, however, have reported significant relationships between spectral indices, including dNBR, and belowground consumption measurements from field sites in boreal ecosystems (Hudak et al., 2007; Verbyla and Lord, 2008; Rogers et al., 2014). Rogers et al. (2014) also found a relatively strong correlation between field measurements of aboveground and belowground consumption, which partly explained the observed relationship between dNBR and belowground consumption. Effective use of dNBR and other remote-sensing observations requires careful integration with other driver data and calibration with field observations that span a wide range of environmental conditions.

The day of burning within the fire season covaries with the depth of burning in the ground layer, and this temporal information may aid prediction of belowground consumption (Turetsky et al., 2011; Kasischke and Hoy, 2012). Convolving burned area detection algorithms with active fire hotspots from the multiple overpasses per day from the Moderate Resolution Imaging Spectroradiometer (MODIS) allows for the development of daily burned area estimates (Parks, 2014; Veraverbeke et al., 2014). Daily burned area products provided evidence that vapor pressure deficit has an important influence on several aspects of fire dynamics including initial spread rate, daily variations in regional burned area, and fire extinction (Sedano and Randerson, 2014). Kasischke and Hoy (2012) developed a daily fire emissions time series to investigate causes of year-to-year variability in carbon consumption for a regional subset of fires during high and low fire years.

Daily burned area and emissions estimates may allow for advances in studies investigating the composition and transport of aerosols and greenhouse gases, fire behavior, or fire modeling. No fire emissions product calibrated using field observations currently exists for use in studying these processes with continuous spatial and temporal coverage, and public availability. Hyer et al. (2007) found that emissions from boreal fires averaged over 30-day intervals resulted in a reduction of 80 % of the variance compared to daily and weekly data in a fire aerosol transport simulation. The temporal resolution of emission data is especially important for boreal fires since they often reach most of their burned area in only a couple of days when the spatiotemporal patterns of ignitions and fire weather optimally coincide (Abatzoglou and Kolden, 2011; Sedano and Randerson, 2014). The representation of extreme fire-weather periods and their influence on burned area in models may allow for more accurate predictions of interannual and decadal changes in the fire regime caused by climate warming (Jin et al., 2014). High resolution emission time series may also improve knowledge about differences in composition of aerosols and trace gases originating from flaming and smoldering stages of combustion (Yokelson et al., 2013) as well as allowing for better prediction of human health impacts in downwind areas (Yao and Henderson, 2014). More fundamentally, daily burned area

estimates are critical for quantitatively examining landscape and weather controls on fire spread rates and severity.

In this paper we describe the creation of a high resolution time series of fire emissions appropriate for investigating many of the fine-scale fire dynamics questions described above. We created a continuous daily time series of fire emissions during 2001–2012 with a spatial resolution of 450 m for the state of Alaska. The combined time span, time step, spatial resolution, spatial domain and calibration with field observations of this product makes it suitable for use in many atmospheric studies, and unique from other published estimates. To estimate carbon consumption at each location (kg C m^{-2} burned area), we developed multiplicative regression models that capture some of the variability in field measurements using gridded environmental variables, including post-fire remote-sensing observations of severity. Our approach also includes uncertainty estimates derived from the fit of our model with the field observations, and includes components associated with our scaling approach used to provide region-wide spatial coverage. The derived daily burned area and carbon emissions product, referred to as the Alaskan Fire Emissions Database (AKFED), is the first wall-to-wall multi-year database with daily temporal resolution that is calibrated using field observations for Alaska and is publicly available. In our analysis, we compared our model estimates with other regional and global biomass burning products from WFEIS and GFED3s. We also show that the set of field observations used does not adequately sample burned area in open forests with sparse tree cover. Since these forests tend to have lower levels of carbon consumption, adjusting for this bias yields lower regional means than what would be inferred directly from the existing set of observations.

2 Spatiotemporal domain and data

2.1 Spatiotemporal domain

The spatial domain covers the area between 58 and 71.5° N, and 141 and 168° W. This represents almost the entire mainland of Alaska with exclusion of the southern part of the Alaska Peninsula and Southeast Alaska, west of British Columbia (Fig. 1). The temporal domain of the study includes the years 2001–2012. Most Alaskan fires occur in the interior of the state, which consists of a mosaic of vegetation types (Fig. S1 in the Supplement). Black spruce forest dominates on cold, poorly drained, north-oriented or lowland sites, whereas white spruce and deciduous species (mainly aspen and birch) prevail on warmer, better drained, south-oriented sites without permafrost (Viereck, 1973; Bonan, 1989). Grass- and shrubland ecosystems occur in early successional stands, poorly drained sites, steep slopes and at and above the treeline. The vegetation mosaic in interior Alaska is constantly reshaped by the occurrence of fire and subse-

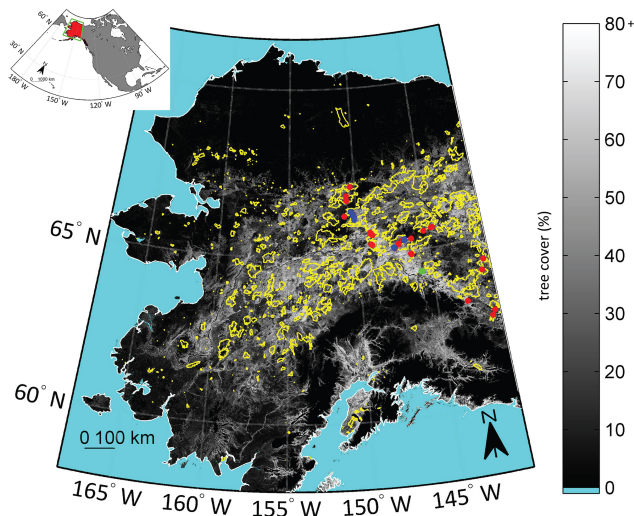


Figure 1. Fires that occurred in the study area between 2001 and 2012 (yellow perimeters) from the Alaska Large Fire Database. The background tree cover map is the Moderate Resolution Imaging Spectroradiometer Vegetation Continuous Fields product (MOD44B, Hansen et al., 2003) for the year 2000. The colored dots represent the location of field plots from Turetsky et al. (2011) (red), Bobby et al. (2010) (blue) and Rogers et al. (2014) (green). Note that at the scale of the map, some field plot locations overlap due to their close proximity to each other.

quent post-fire succession. Fewer fires occur in the tundra regions in the north and at the western coastal areas of the state; however, the 2007 Anaktuvuk River fire on the North Slope is the largest tundra fire on record (Jones et al., 2009; Mack et al., 2011; Kolden and Rogan, 2013).

2.2 Field data

We assembled field data of depth of burn from three different publications (Boby et al., 2010; Turetsky et al., 2011; Rogers et al., 2014). Due to limited data availability for other land-cover types than black spruce (five plots in Rogers et al., 2014), we focused on black spruce plots, and we retained all plots burned since 2000 for which cloud-free 1-year-post-fire dNBR observations were available in the Monitoring Trends in Burn Severity (MTBS, Eidenshink et al., 2007) database, resulting in a total of 126 plots (Table S2 in the Supplement). The location of the field plots is given in Fig. 1. Bobby et al. (2010) and Rogers et al. (2014) provided a direct estimate of the belowground carbon consumption representing 39 plots. Both studies sampled multiple soil cores (11 in Bobby et al., 2010, and 6 in Rogers et al., 2014) in a 2 m × 30 m transect in each plot. These studies estimated pre-fire carbon stocks from control sites that were chosen to match the conditions of the burned sites. These studies used measurements of adventitious roots (Kasischke and Johnstone, 2005; Kasischke et al., 2008) within the soil column in combination with bulk density and carbon concentrations

to calculate the pre-fire soil carbon stock. Belowground carbon consumption was defined as the difference between the pre- and post-fire carbon stocks. These plots, except for one in Bobby et al. (2010), also included an estimate of aboveground carbon consumption. Bobby et al. (2010) and Rogers et al. (2014) both estimated aboveground carbon stock using allometric equations and diameter-at-breast height measurements of individual trees. Both studies multiplied visual estimates of percentage consumption of the aboveground carbon pools to derive aboveground carbon consumption. Turetsky et al. (2011) aggregated depth of burn data from multiple methods including the adventitious roots technique, burned–unburned site pairings, and combustion rods, with varying numbers of measurements per site. For the Turetsky et al. (2011) plots, belowground carbon consumption was calculated from depth of burn measurements using separate, region-wide mean soil-carbon accumulation curves for lowland, upland, and slopes with south (S), north (N), and east or west (EW) aspect (Fig. S2). We used a digital elevation model (Sect. 2.3.3) resampled to 450 m resolution for assigning the topographic classes to the field plots. Concave flat (slope $\leq 2\%$) areas were classified as lowland (L), convex flat areas were as upland (U). Sloped terrain was categorized as N aspect (aspect ≥ 315 or $< 45^\circ$), S aspect (aspect ≥ 135 and $< 225^\circ$), and E or W aspect (aspect ≥ 45 and $< 135^\circ$, or ≥ 225 and $< 315^\circ$). More detailed description of the field sites and data acquisition can be found in the respective publications. We also note that the sampling approach used by Rogers et al. (2014) was designed to enable comparisons with 30 m geospatial layers. To account for potential georegistration errors, their plots were therefore selected within 100 m × 100 m patches that were relatively homogeneous in pre- and post-fire characteristics.

2.3 Geospatial data

2.3.1 Alaska Large Fire Database (ALFD)

The Alaska Large Fire Database (ALFD) currently contains fire perimeters for the state of Alaska from 1940 through the present (downloaded from <http://afsmaps.blm.gov/imf/imf.jsp?site=firehistory>, last access: 14 May 2015). The database receives yearly updates. The reliability of the database increases through time as mapping technologies advanced; since the 1980s, consistent mapping with high quality and few omissions has been achieved (Kasischke et al., 2002, 2011). For our study, we extracted the fire perimeters of the years 2001–2012 from the ALFD (Fig. 1).

2.3.2 Active fire data

The Global Monthly Fire Location Product (MCD14ML) contains geographic location and time for each fire pixel detected by MODIS on Terra (launched in December 1999) and Aqua (launched in May 2002). Additional information

on brightness temperature, fire radiative power, scan angle and detection confidence is also provided. The product is based on a contextual active fire algorithm that exploits the strong emission in the mid infrared region from fires (Giglio et al., 2003, 2006). We extracted the fire detections from all confidence levels for our domain for the months May–September, the months of the fire season, for all years. MODIS on Terra experienced an extended outage during our study period from 16 June through 2 July 2001 (Giglio et al., 2013).

2.3.3 Environmental variables

Ground layer consumption by fire depends on the amount of available dry fuels, which is determined by thickness, density and moisture content of the organic layer. After an extensive literature review, we selected a set of environmental variables to predict ground layer consumption over the landscape (Table 1). The selected environmental variables were elevation, slope, northness (defined as the cosine of the aspect), tree cover, day of burning, and dNBR.

Topography is a good proxy of site conditions for several reasons. Elevation influences organic layer thickness, carbon density, drainage and permafrost thaw by means of its control on climate. At higher elevations the seasonal permafrost thaw starts later (Kasischke and Johnstone, 2005; Kasischke and Hoy, 2012). Uplands generally have shallower organic layers with a slightly higher carbon density than lowlands (Kane et al., 2005, 2007; Turetsky et al., 2011). Uplands are generally also better drained than lowlands (Barrett et al., 2010; Kasischke and Hoy, 2012). Steep terrain is better drained than flat land, but above a certain threshold steepness limits the establishment of trees resulting in shallower organic layers at steeper sites (Hollingsworth et al., 2006). In crown fire ecosystems, fire severity tends to increase with steepness when the wind direction aligns upslope (Rothermel, 1972; Pimont et al., 2012; Lecina-Diaz et al., 2014), and this may also affect ground layer consumption. North-oriented slopes are wetter and colder than south-faced slopes and have thicker, less dense organic layers (Kane et al., 2007; Turetsky et al., 2011). Here we derived elevation, slope and northness from the Advanced Spaceborne Thermal Emission and Reflection Radiometer Global Digital Elevation Model Version 2 (ASTER GDEM 2, Tachikawa et al., 2011). The ASTER GDEM 2 is a 30 m elevation model retrieved from ASTER stereo-pair images.

Pre-fire tree cover is closely related to site productivity and stand age, and thus influences organic layer thickness, density and moisture content (Kasischke and Johnstone, 2005; Beck et al., 2011b; Rogers et al., 2013). Tree cover generally increases with stand age and better drainage conditions (Beck et al., 2011b; Rogers et al., 2013). Tree cover also is directly related to the amount of biomass available for aboveground consumption, which has been shown to correlate reasonably well with belowground consumption within a single

fire (Rogers et al., 2014). For the comparison with the field plots, we used 30 m tree cover data from the Landsat-based tree cover continuous field product for the year 2000 (Sexton et al., 2013). For the statewide-extrapolation, tree cover was downloaded from the annual Terra MODIS Vegetation Continuous Fields Collection 5 product at 250 m resolution for the years 2000–2010 (MOD44B, Hansen et al., 2003). The generation of the MOD44B product was discontinued after 2010, and we therefore used the tree cover layer of the year 2010 as pre-fire tree cover for the year 2012.

The day of burning in the season covaries with the mean depth of the active layer, and thus may be related to the amount of dry ground fuels available for burning (Turetsky et al., 2011; Kasischke and Hoy, 2012). We assigned the day of burning for each pixel based on the MODIS active fire observations. We found that the nearest neighbor variant of the inverse distance weighting technique, in which the pixel is assigned the value of the closest active fire detection excluding scan angles larger than 40°, performed best and with a within-1-day accuracy for most pixels (Fig. S3). The resulting progression maps were binned with a daily time step, at local solar time.

We investigated the dNBR as an explanatory variable in our carbon consumption model because extensive literature suggests that it may have some predictive power in boreal forest ecosystems. For the comparison with the field plots, 30 m dNBR data was retrieved from the Landsat-based Monitoring Trends in Burn Severity database (MTBS, Eidenshink et al., 2007). For the statewide-extrapolation, we calculated NBR from MODIS surface reflectance data in the near infrared (NIR, centered at 858 nm) and short-wave infrared (SWIR, centered at 2130 nm) bands: $NBR = (NIR - SWIR) / (NIR + SWIR)$. We used the surface reflectance data contained in the 16-day Terra MODIS Vegetation Indices Collection 5 product at 500 m resolution for the years 2000–2013 (MOD13A1, Huete et al., 2002). To account for cloudy observations in single MODIS composites, we created summer NBR composites using the five 16-day composites between days of the year 177 and 256. We only used good data as indicated by the MOD13A1 quality flags. NBR values were calculated as the mean of all available good observations within the five composites. dNBR was calculated using the 1-year pre- and post-fire NBR layers. Within the MTBS database, we also only considered 1-year-post-fire dNBR information. This minimized potential differences in the interpretation of dNBR values from different post-fire years (Veraverbeke et al., 2010; Rogers et al., 2014).

The above six variables (elevation, slope, northness, tree cover, day of burning and dNBR) were targeted to develop the belowground carbon consumption model. dNBR and tree cover were used as predictors of aboveground carbon consumption.

Table 1. Environmental variables selected to predict ground layer consumption by fire in black spruce forest. The pre-fire tree cover and dNBR layers were also used to predict the aboveground carbon consumption.

Variable	Rationale	Data
Elevation (m)	Elevation influences soil organic layer thickness, carbon density, drainage conditions and seasonal timing of active-layer thaw (Kane et al., 2005, 2007; Kasischke and Johnstone, 2005; Barrett et al., 2010; Kasischke and Hoy, 2012)	ASTER GDEM 2 (Tachikawa et al., 2011)
Slope (°)	Slope regulates drainage conditions, organic layer thickness and fire behavior. Sloped terrain is generally better drained than flat terrain (Barrett et al., 2011). Steepness of the terrain regulates tree establishment (Hollingsworth et al., 2006) and fire spread rates and severity (Rothermel, 1972).	derived from ASTER GDEM 2
Northness – cosine of aspect	Northness regulates drainage conditions, organic layer thickness and carbon density. Wetness increases with northness, and solar insolation decreases with increasing northness. North-oriented slopes are wetter and colder than south-faced slopes and have thicker, less dense organic layers (Kane et al., 2007; Turetsky et al., 2011).	derived from ASTER GDEM 2
Pre-fire tree cover (%)	Pre-fire tree cover determines the available biomass for aboveground consumption. Aboveground consumption relates to belowground consumption (Rogers et al., 2014). Pre-fire tree cover is also a proxy of stand age, and thus of the thickness, density and wetness of the soil organic layer (Kasischke and Johnstone, 2005; Beck et al., 2011b; Rogers et al., 2013).	Tree cover continuous fields: 30 m: Sexton et al. (2013) 250 m: Hansen et al. (2003)
Day of burning	Day of burning influences the dryness of the soil organic layer during the season (Turetsky et al., 2011; Kasischke and Hoy, 2012)	derived from MODIS active fire data
dNBR	dNBR assesses pre-/post-fire changes in near and shortwave infrared reflectance, which relate to changes in vegetation abundance, charcoal deposition and soil exposure (López García and Caselles, 1991; van Wagtenonk et al., 2004; Key and Benson, 2006)	30 m: MTBS (Eidenshink et al., 2007) 500 m: derived from MODIS surface reflectance

ASTER GDEM 2: Advanced Spaceborne Thermal Emission and Reflection Radiometer Global Digital Elevation Model Version 2 (downloaded from <http://reverb.echo.nasa.gov>, last access: 14 May 2015),

dNBR: differenced normalized burn ratio,

MODIS: Moderate Resolution Imaging Spectroradiometer,

MTBS: Monitoring Trends in Burn Severity (downloaded from <http://www.mtbs.gov/>, last access: 14 May 2015),

Tree cover data downloaded from <http://glcf.umd.edu/data/landsat/Treecover/> (30 m), and <http://reverb.echo.nasa.gov> (500 m), MODIS surface reflectance data from <http://reverb.echo.nasa.gov>, MODIS active fire data from <ftp://fuoco.geog.umd.edu/modis> (all last access: on 14 May 2015).

2.3.4 Land-cover data

We used the Fuel Characteristic Classification System (FCCS, Ottmar et al., 2007; Riccardi et al., 2007) layer of the year 2001 at 30 m to represent land-cover in the study area (downloaded from <http://landfire.cr.usgs.gov/viewer/>, last access: 14 May 2015). The FCCS is a national effort by

the US Forest Service to provide a fuel type classification that is compiled from literature, inventories, photo series and expert opinion (Ottmar et al., 2007; Riccardi et al., 2007). For Alaska, the layer is available for the years 2001 and 2008. Since less than 1 % of re-burning occurred during the period of our study (2001–2012), we decided to only use

the 2001 layer. We aggregated the fuel types into five land-cover classes: black spruce, white spruce, deciduous, tundra–grass–shrub and non-vegetated (Table S1, Fig. S1). Other than the National Land Cover Database in Alaska (Stehman and Selkowitz, 2010), the FCCS layer discriminates between black and white spruce fuel types. The uncertainty of the FCCS layer in Alaska has not been formally assessed.

3 Methods

AKFED provides daily burned area and carbon emissions for the state of Alaska between 2001 and 2012 at 450 m resolution. Since unburned islands are not fully accounted for within perimeters (Kasischke and Hoy, 2012; Kolden et al., 2012; Rogers et al., 2014; Sedano and Randerson, 2014), and some small fires are not accounted for outside the perimeters (Randerson et al., 2012), we developed a burned area mapping approach that screened dNBR values within the ALFD perimeters and in the vicinity of active fire pixels outside the perimeters (Sect. 3.1).

The carbon consumption model was formulated for black spruce based on the relationship between the observed carbon consumption at the field locations and the environmental variables. We extracted the pixel values of elevation, slope, northness, pre-fire tree cover and dNBR at 30 m at the location of the field plots. The day of burning was assigned from the nearest active fire observation.

To extrapolate the model in space and time, we used a spatial resolution of 450 m. This is the multiple of 30 m closest to the exact 463 m native resolution of the MOD13A1 product used to derive the dNBR layers (Masuoka et al., 1998). This spatial resolution facilitated spatial averaging of 30 m DEM (digital elevation model), tree cover, dNBR and land-cover data. The decision to extrapolate the model at this resolution was driven by data availability. We aimed at complete spatial coverage. Even with current efforts such as MTBS and the Web-Enabled Landsat Data (WELD, Roy et al., 2010), initial exploration of these data sets indicated that complete Landsat dNBR coverage for every burned pixel was still partly constrained by clouds, smoke, snow and gaps caused by the Landsat 7 scan line corrector failure.

Elevation, aspect and northness were spatially averaged from the native 30 m resolution of the ASTER GDEM 2 to the 450 m resolution. Similarly, the MOD44B tree cover product was spatially averaged from its native resolution to the 450 m resolution. The day of burning was also obtained at this grid resolution. To account for other land-cover types than black spruce, the aggregated FCCS product was rescaled to 450 m in a way that every pixel at 450 m contained the percentage of black spruce, white spruce, deciduous, tundra–grass–shrub and non-vegetated land (Fig. S1). All analyses were performed within the Albers equal area projection for Alaska (central meridian: 154° W, standard parallel 1: 55° N, standard parallel 2: 65° N, latitude of origin: 50° N) with

North American Datum 1983 (NAD83). An overview of the workflow is given in Fig. 2.

We compared the annual burned area and carbon emissions estimates derived from AKFED with those from WFEISv0.4 (French et al., 2014) and GFED3s (Randerson et al., 2012), two continental to global-scale modeling systems. Since WFEIS and GFED3s were not directly calibrated with region specific field data, comparisons with AKFED may be instructive for improving carbon consumption in boreal forest ecosystems. We used the MCD64A1 burned area product (Giglio et al., 2009) within the WFEIS emissions calculator. MCD64A1 was also the burned area layer within GFED3s (Randerson et al., 2012). A small amount of burned area (8 %) associated with fires outside the MCD64A1 burned areas, are accounted for in Alaska in the GFED3s approach (Randerson et al., 2012). AKFED burned area has conceptual similarities with this latter approach.

3.1 Daily burned area mapping (450 m)

Annual burned area maps at 450 m were derived by applying a threshold on the dNBR values of pixels within the perimeters of the ALFD and outside the perimeters but within 1 km of an active fire pixel. If any fraction of the 450 m pixel was covered by a fire perimeter polygon, then this pixel was considered in the perimeter. Pixels with a dNBR value larger than 0.15 were classified as burned. The dNBR threshold was determined based on the dNBR variability that exists within unburned pseudo-invariant pixels (100 % barren pixels at 450 m, FCCS code 931). We found, as expected, that the mean dNBR was close to 0 (0.01). The standard deviation of the distribution equaled 0.15. By selecting this value as our threshold for the burned area mapping, we aimed to minimize commission errors; however, we recognize that this may have incurred a small omission error for pixels that were only partially burned and/or burned with low severity. The threshold value we used was the same as the one applied by Sedano and Randerson (2014) who used a similar burned area mapping approach within ALFD perimeters. All burned pixels were assigned a day of burning from the detection time of the nearest active fire observation excluding observations with view zenith angles higher than 40° (Fig. S3).

3.2 Carbon consumption model (30 m)

We aimed to separately predict below- and aboveground carbon consumption based on the relationships between field plot data and environmental variables at 30 m (elevation, slope, northness, pre-fire tree cover, day of burning and dNBR). We focused on modeling carbon consumption; however, we also reported the results of the depth of burn model because of this variable is widely measured and analyzed in the literature (e.g., Barrett et al., 2010, 2011; Turetsky et al., 2011; Genet et al., 2013). We investigated two modeling techniques to formulate a carbon prediction model. The

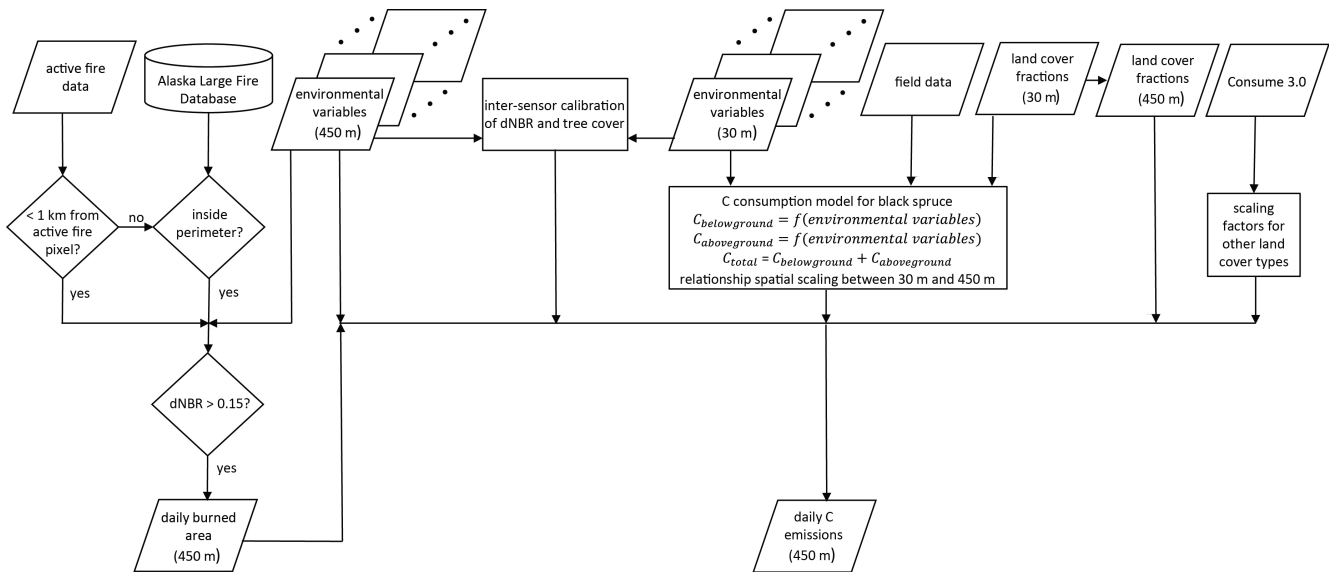


Figure 2. Workflow used to obtain daily burned area and carbon emissions in the Alaskan Fire Emissions Database (AKFED). dNBR: differenced normalized burn ratio.

first technique was multiplicative nonlinear regression. This technique is based directly on the interpretation of empirical relationships that may exist between the environmental variables and the carbon consumption field data. Multiplicative nonlinear regression has demonstrated to be effective in a similar application to predict fire occurrence and size in Southern California (Jin et al., 2014). The second technique was gradient boosting of regression trees. We applied this technique because previous work indicated that it may have value in predicting depth of burning in boreal black spruce forests (Barrett et al., 2010, 2011). Gradient boosting is a machine learning technique, which produces a prediction model in the form of an ensemble of, in our case, multiple regression trees. We parameterized the gradient boosting of regression trees with the requirement that each leaf included at least 10 % of the data per leaf and using 50 weak learner trees. Both multiplicative nonlinear regression and gradient boosting of regression trees allow for nonlinear relationships between the dependent and independent variables, and interactions between the independent variables. We opted to use the multiplicative nonlinear regression model for our study because we found it to considerably outperform the gradient boosting model in predicting observations that were not used to train the models (Fig. S4).

3.3 Daily carbon emissions, 2001–2012 (450 m)

Once optimized, we extrapolated the carbon consumption model over the spatiotemporal domain of the study at 450 m resolution. To do so, we first quantified the linear relationship between Landsat and MODIS dNBR and tree cover (Fig. S5). The resulting regression equations were applied to the MODIS-derived dNBR and tree cover layers to allow

direct application in the carbon consumption model that was optimized using Landsat data.

Due to data paucity of carbon consumption observations in other land-cover types than black spruce, we developed separate consumption models for these ecosystems that drew upon the data-driven approach for black spruce. Deciduous and white spruce stands generally have higher aboveground and lower belowground fuel loads (Kasischke and Hoy, 2012; Rogers et al., 2014). We assumed that carbon consumption in these land-cover types was controlled by the same variables as from the black spruce consumption model. However, we multiplied the estimates derived from our black spruce-based equations by consumption ratios for above- and belowground deciduous and white spruce stands that were developed using the Consume 3.0 fuel consumption model (Ottmar et al., 2006; Prichard et al., 2006) (Fig. S6). Consumption estimates derived from the black spruce model were multiplied with the consumption ratios proportional to the land-cover fractions within each pixel. For the state-wide extrapolation over pixels classified as tundra–grass–shrub and non-vegetated, we used the model derived for black spruce. The mean tree cover value of all 30 m tundra–grass–shrub and non-vegetated pixels within the ALFD perimeters between 2001 and 2012 was 11 % (standard deviation, SD, = 14 %).

We also quantified the influence of applying the nonlinear multiplicative model (developed at 30 m resolution) using data with a spatial resolution of 450 m to enable state-wide coverage. For this analysis, we selected all cloud-free 1-year-post-fire observations of the large fire year 2004 from MTBS. We co-registered these with all good-quality observations from the Landsat tree cover layer, the 30 m DEM,

30 m progression maps (derived using the nearest neighbor approach), and the 30 m land-cover map. We then estimated carbon consumption at 30 m and averaged the resulting carbon consumption over 450 m pixels for those 450 m pixels that had complete 30 m dNBR and tree-cover coverage. For these same pixels, we also first averaged all 30 m input layers (dNBR, tree cover, DEM, progression, and land cover) to 450 m, and then estimated carbon consumption at 450 m resolution.

3.4 Uncertainty

We adopted a Monte Carlo approach to quantify uncertainties in AKFED. We identified four main sources of uncertainty. The first source originates from the unexplained variance in the black spruce consumption model. The uncertainty estimate from the black spruce consumption model was derived quantitatively from the regression model and varied from pixel to pixel as a function of the input variables. The other sources of uncertainty were related to assumptions and data required to extrapolate the model over Alaska. These included uncertainties in the spatial scaling of a model developed with 30 m data at 450 m resolution, the land-cover classification, and assumptions made for deriving carbon consumption for other land-cover types than black spruce. Uncertainties derived from the spatial scaling were quantitatively estimated using the approach described in Sect. 3.3. For the land-cover classification, because of a lack of quantitative information associated with the classification uncertainty, we assumed a best-guess standard deviation uncertainty of 20% of the pixel-based black spruce fraction. We also assigned a best-guess uncertainty (one SD) of 20% of the value range for the factors developed to estimate carbon consumption in other land-cover types than black spruce (Fig. S6). We ran 1000 simulations at each pixel that burned between 2001 and 2012 in which we randomly adjusted the regression model estimates, the land-cover fractions, and scaling relationships using the uncertainty information described above. We conducted three separate Monte Carlo simulation analyses for belowground, aboveground and total carbon consumption.

4 Results

4.1 Carbon consumption model

The relationship between the depth of burn and the individual environmental variables was strongest for dNBR and tree cover ($R^2_{\text{adjusted}} = 0.25$, $p < 0.001$), with both relationships modeled using exponential response functions (Fig. S7). Depth of burn responded with a relatively strong Gaussian relationship to elevation ($R^2_{\text{adjusted}} = 0.24$, $p < 0.001$), with the deepest burning occurring in the mid-elevation range between 300 and 600 m. A weak relationship was found for slope ($R^2_{\text{adjusted}} = 0.05$, $p < 0.05$), and no relationship was

observed for day of burning or northness. The strongest individual predictors for belowground carbon consumption were day of burning ($R^2_{\text{adjusted}} = 0.09$, $p < 0.001$), slope ($R^2_{\text{adjusted}} = 0.08$, $p < 0.01$) and dNBR ($R^2_{\text{adjusted}} = 0.06$, $p < 0.01$). Northness ($R^2_{\text{adjusted}} = 0.04$, $p < 0.05$), elevation ($R^2_{\text{adjusted}} = 0.04$, $p < 0.05$), and tree cover ($R^2_{\text{adjusted}} = 0.03$, $p < 0.05$) had a weaker influence (Fig. S8). The aboveground carbon consumption demonstrated stronger, also exponential, relationships with pre-fire tree cover ($R^2_{\text{adjusted}} = 0.53$, $p < 0.001$) and dNBR ($R^2_{\text{adjusted}} = 0.23$, $p < 0.001$) variables (Fig. S9).

The optimized multiplicative nonlinear model for the depth of burn and belowground carbon consumption in black spruce forest based on the field and 30 m data was formulated as follows:

$$\text{depth}_{30\text{m}} \text{ or } C_{\text{belowground, 30m}} = c_1 + c_2 \cdot e^{c_3 \cdot \text{dNBR}} \cdot e^{c_4 \cdot \text{tc}} \cdot e^{c_5 \cdot \text{DOY}} \cdot e^{-\frac{(\text{elev}-c_6)^2}{2 \cdot c_7}}, \quad (1)$$

where $c_{1,\dots,7}$ are the optimized coefficients, dNBR is the differenced normalized burn ratio, tc is the pre-fire tree cover, DOY is the day of the year, and elev is the elevation. Two separate models were developed for depth of burn and belowground carbon consumption using Eq. (1). The depth of burn model yielded a R^2_{adjusted} of 0.40 with a median absolute residual of 3.65 cm ($p < 0.001$) (Fig. 3a). For belowground carbon consumption, the model obtained a R^2_{adjusted} of 0.29 with a median absolute residual of 1.18 kg C m⁻² ($p < 0.001$) for belowground carbon consumption (Fig. 3c). Inclusion of slope and northness did not improve the performance of the two models.

The aboveground carbon consumption in black spruce forest was modeled as a multiplicative exponential model of the 30 m dNBR and pre-fire tree cover variables:

$$C_{\text{aboveground, 30m}} = c_1 + c_2 \cdot e^{c_3 \cdot \text{dNBR}} \cdot e^{c_4 \cdot \text{tc}}, \quad (2)$$

where $c_{1,\dots,4}$ are the optimized coefficients. This model had a R^2_{adjusted} of 0.53 with a median absolute residual of 0.12 kg C m⁻² ($p < 0.001$) (Fig. 3e), with a performance similar to the individual relationship between the aboveground carbon consumption and pre-fire tree cover. In the mostly stand-replacing fires that occur in black spruce forest, dNBR did not contribute to the aboveground model. However, we decided to include dNBR to allow for variations in the severity of burning in other land-cover types than black spruce, for example in deciduous stands which often burn less severely and frequently (Viereck, 1973; Cumming, 2001). We found no trends in the residuals of any of the models (Fig. 3b, d and f). The environmental variables used in the carbon consumption models are shown for the spatiotemporal domain in Fig. S10.

Applying the black spruce model at 450 m resolution introduced little systematic bias from the coarser spatial reso-

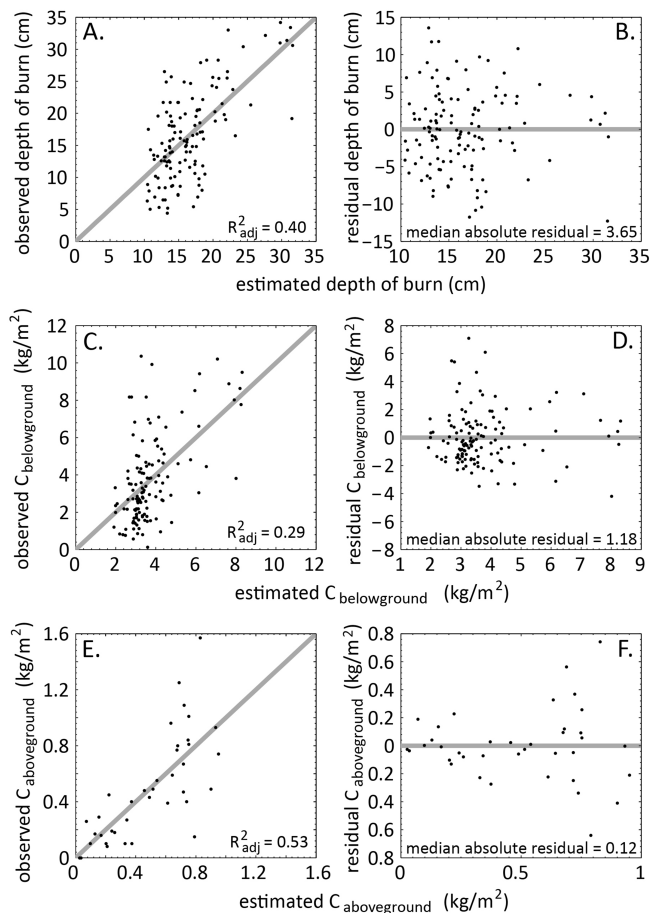


Figure 3. Scatter plots between the observed and estimated (a) depth of burn, (c) belowground and (e) aboveground carbon consumption from the multiplicative nonlinear model, and corresponding regression residuals (b, d and f). The gray line represents the 1 : 1 line in the left panels, and the $y = 0$ line in the right panels. All models were significant at $p < 0.001$.

lution (Fig. S11). Using the consumption ratios derived for white spruce and deciduous cover (Fig. S6) and slope and intercept from the 30 to 450 m scaling analysis (Fig. S11), below- and aboveground carbon consumption at 450 m resolution were calculated as follows:

$$C_{\text{belowground}, 450\text{m}} = -0.005 + 1.015 \cdot (\text{fr}_{\text{bs}} + 0.66 \cdot \text{fr}_{\text{ws}} + 0.31 \cdot \text{fr}_{\text{dec}}) \cdot C_{\text{belowground}, 30\text{m}}, \quad (3)$$

$$C_{\text{aboveground}, 450\text{m}} = 0.023 + 1.077 \cdot (\text{fr}_{\text{bs}} + 1.56 \cdot \text{fr}_{\text{ws}} + 1.75 \cdot \text{fr}_{\text{dec}}) \cdot C_{\text{aboveground}, 30\text{m}}, \quad (4)$$

where fr_{bs} is the fraction of black spruce within the 450 m pixel, fr_{ws} is the fraction of white spruce and fr_{dec} is the fraction of deciduous. The black spruce model was also applied to residual tundra–grass–shrub and non-vegetated parts of each pixel. Before application of Eqs. (3) and (4), the dNBR and tree cover from MODIS were first converted into their Landsat equivalent values using the equations from Fig. S5.

The total carbon consumption was calculated as the sum of the below- and aboveground carbon consumption.

To assess the importance of the individual variables, we compared all possible multiplicative regression models with two or more input variables for the depth of burn and belowground carbon consumption (Fig. 4). For the depth of burn model, elevation was the most important explanatory variable. For example, 2-variables models combining elevation with day of burning and dNBR performed better than the 3-variables models that excluded elevation. For the belowground carbon consumption model, the day of burning variable was crucial. All 2-variables models combining day of burning with any of the other variables performed better than the 3-variables models that excluded day of burning.

4.2 Daily burned area and carbon emissions, 2001–2012

The total carbon emissions and uncertainty for the spatiotemporal domain are shown in Figs. 5 and 6. Daily carbon emissions over the entire spatial domain were primarily driven by daily burned area (Fig. 6); however, there was considerable spatial variability in carbon consumption (Fig. 5). Annual burned area in Alaska from AKFED ranged between 37 and 2295 kha year⁻¹ between the years 2001 and 2012, resulting in a carbon emission range between 1 and 69 Tg year⁻¹ (Fig. 7a). 1 % of the burned area was mapped from active fire detections outside the perimeters, whereas 18 % of the pixels within the ALFD perimeters were mapped as unburned after dNBR screening. 2004 (2295 kha), 2005 (1669 kha), 2009 (1046 kha) and 2002 (739 kha) were the largest fire years. More than 50 % of the burned area between 2001 and 2012 burned in 53 single days (Fig. 6). Most of the burning occurred in July and August (Fig. 7b). The seasonal pattern of carbon emissions generally followed the same seasonal pattern as the burned area. However, carbon consumption increased by a small amount later in the season. Mean annual carbon consumption increased slightly with total annual burned area (Fig. 8) and mean carbon consumption per fire and fire size were positively correlated ($r = 0.24$, $p < 0.001$). Mean dNBR per fire was correlated with fire size (Spearman $r = 0.63$, $p < 0.001$), and dNBR averaged over the fire season was correlated with annual burned area (Spearman $r = 0.73$, $p < 0.05$). Most of the burned area occurred in black spruce and white spruce ecosystems (61 %), followed by tundra–grass–shrub ecosystems (23 %), deciduous forests (14 %), and non-vegetated areas (2 %), with an overall mean tree cover of 32 %.

The median total carbon consumption in AKFED for all burned pixels between 2001 and 2012 was 2.54 kg C m⁻², with the majority originating from belowground losses (median = 2.32 kg C m⁻²) (Fig. 9a). The median aboveground carbon consumption was 0.18 kg C m⁻². The median belowground carbon consumption was higher in burned pixels that had a vegetation cover of 100 % black spruce (median

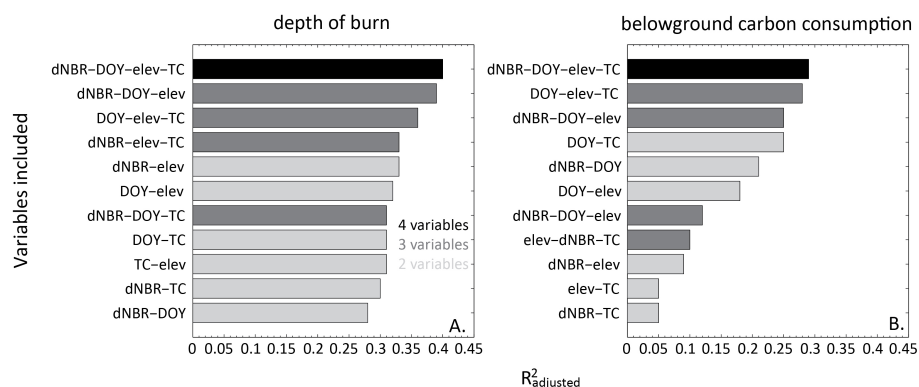


Figure 4. Relative importance of variables assessed from the nonlinear multiplicative models using all different combinations of two or more variables for (a) depth of burn and (b) belowground carbon consumption. Since only two variables were included in the aboveground carbon consumption model, no similar analysis was performed for aboveground carbon consumption. dNBR: differenced normalized burn ratio, DOY: day of the year, tc: tree cover, elev: elevation.

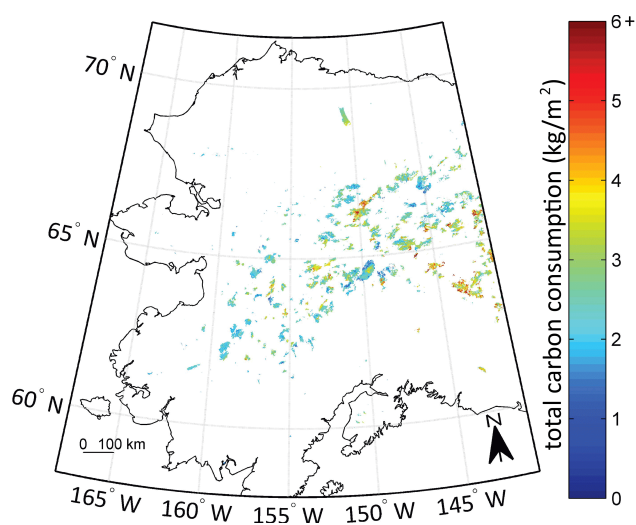


Figure 5. Total pyrogenic carbon consumption estimated from the Alaskan Fire Emissions Database between 2001 and 2012.

$= 2.67 \text{ kg C m}^{-2}$) (Fig. 9b). However, belowground carbon consumption estimates for black spruce were lower than those observed in the field data median $= 3.1 \text{ kg C m}^{-2}$). The field data also had a higher median elevation, tree cover and dNBR compared to the distribution of the burned area between 2001 and 2012 (Fig. 10).

Annual burned area from AKFED, WFEIS and GFED3s were fairly similar (Table 2). Relative to the AKFED burned area estimates between 2001 and 2010, WFEIS burned area estimates were about 10 % lower, and GFED3s estimates approximately 2 % lower. Annual carbon emissions estimates showed larger differences. WFEIS carbon emissions estimates were approximately 142 % higher than AKFED between 2001 and 2010, and GFED3s carbon emissions estimates were approximately 13 % lower than AKFED. Carbon consumption estimates of WFEIS were approximately 168 %

higher than AKFED, whereas GFED3s carbon consumption estimates were approximately 12 % lower than AKFED between 2001 and 2010. No significant correlations were found between year-to-year variations in mean carbon consumption estimates from the different models.

4.3 Uncertainties

Uncertainty in total carbon consumption originated primarily from the belowground fraction (Fig. 11). The region-wide standard deviation of the 1000 simulations that included all uncertainty sources was 0.50 kg C m^{-2} for total carbon consumption. Region-wide below- and aboveground uncertainties from all sources were 0.47 and 0.14 kg C m^{-2} . The black spruce model was the main source of uncertainty, followed by the land-cover classification. The scaling factors developed to derive carbon consumption in other land-cover types than black spruce and spatial scaling introduced smaller uncertainties.

5 Discussion

5.1 Burned area

Our results corroborate previous work highlighting the importance of unburned islands, which amounted to 18 % of the fire perimeters. This value is close to the estimates of 14, 15, 17, and 20 % reported by Kolden et al. (2012), Sedano and Randerson (2014), Rogers et al. (2014) and Kasischke and Hoy (2012) for fires in interior Alaska. Burned area and emissions peaked in July and August and extended later in the fire season than what has been previously reported for burning before the 2000s (Kasischke et al., 2002) (Fig. 7b). This tendency towards late-season burning was found for the four largest fire years that occurred during the study period (2002, 2004, 2005 and 2009) (Fig. 6) and can be attributed to

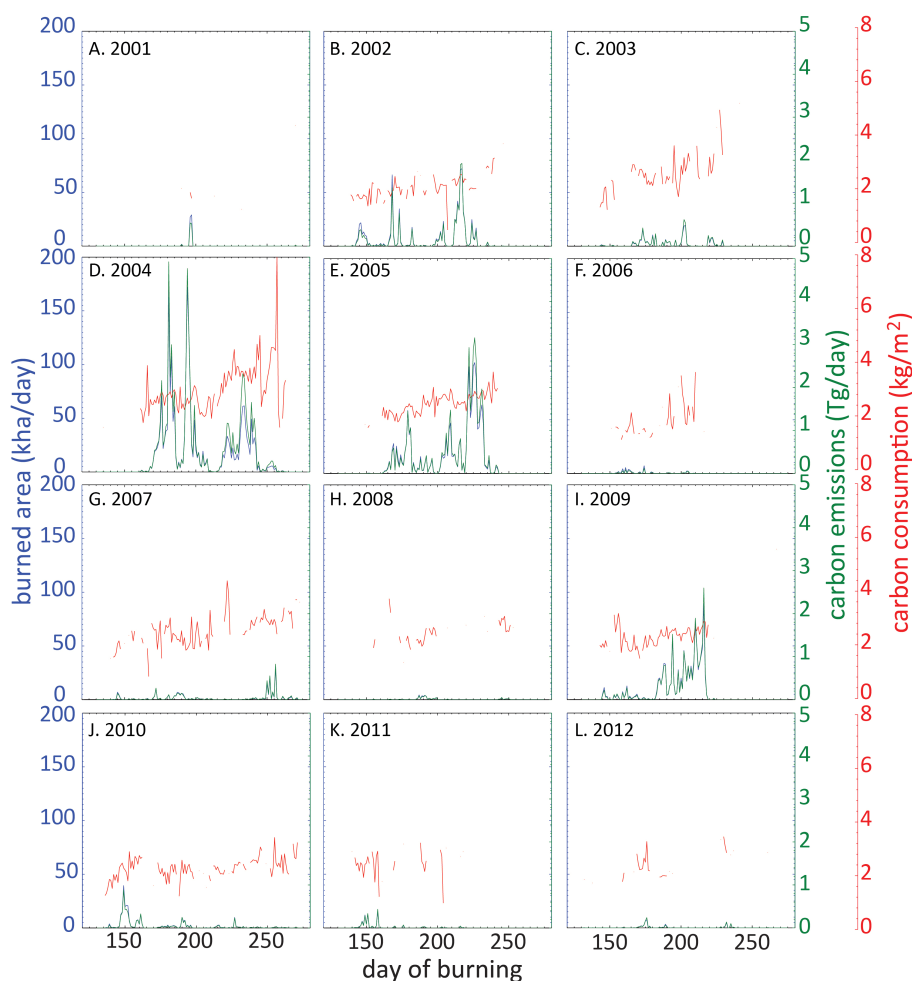


Figure 6. Daily burned area, carbon consumption and emissions derived from the Alaskan Fire Emissions Database for the years 2001–2012.

Table 2. Annual burned area, carbon emissions, and mean carbon consumption between 2001 and 2010 from the Alaskan Fire Emissions Database (AKFED), the Wildland Fire Emissions Information System (WFEIS), and the Global Fire Emissions Database version 3s (GFED3s). Values were extracted for the domain between 58 and 71.5° N, and 141 and 168° W. We used the MCD64A1 burned area product and the default parameters within the WFEIS emissions calculator (<http://wfeis.mtri.org/calculator>, last access: 14 May 2015). We included both emissions from natural and agricultural fuels.

Year	Annual burned area (kha)			Annual C emissions (Tg)			Mean C consumption (kg m^{-2})		
	AKFED	WFEIS	GFED3s	AKFED	WFEIS	GFED3s	AKFED	WFEIS	GFED3s
2001	61	0	2	1	0	0	1.89	/	2.57
2002	739	595	636	17	46	15	2.27	7.74	2.44
2003	200	188	200	5	10	5	2.74	5.24	2.51
2004	2294	2253	2283	69	167	52	3.03	5.88	2.26
2005	1660	1320	1538	46	102	38	2.76	7.75	2.47
2006	47	68	86	1	3	2	1.76	4.75	2.40
2007	200	130	165	5	8	5	2.63	6.55	2.80
2008	37	24	34	1	2	1	2.37	7.32	1.86
2009	1046	1054	1130	26	77	29	2.51	7.27	2.52
2010	268	283	324	6	16	8	2.25	5.55	2.34
2001–2010	655	592	634	18	43	15	2.72	7.29	2.40

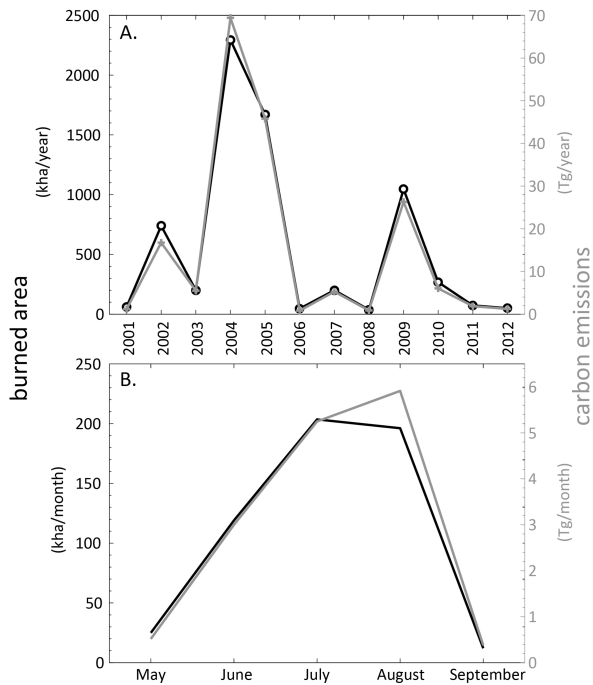


Figure 7. (a) Inter- and (b) intra-annual variability in burned area and carbon emissions in Alaska. In (b), the mean monthly burned area and carbon emissions between 2001 and 2012 were plotted.

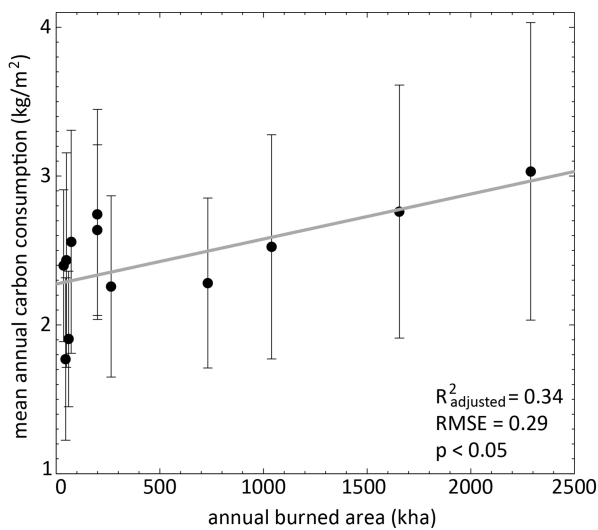


Figure 8. Relationship between annual burned area and mean annual carbon consumption. The error bars represent 1 standard deviation.

the late-season occurrence of weather conditions favorable to fire spread during these large fire years (Hu et al., 2010; Sedano and Randerson, 2014).

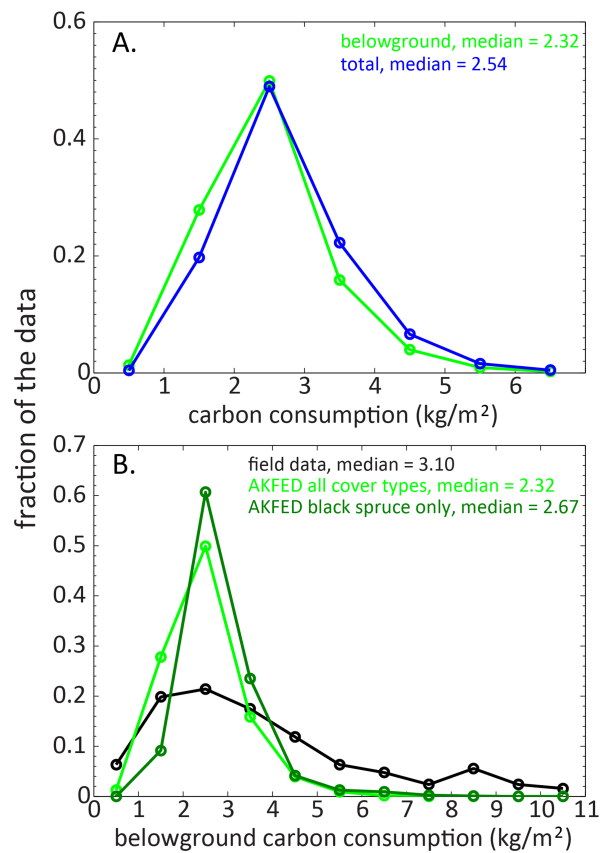


Figure 9. Distribution of (a) belowground, aboveground and total carbon consumption from the Alaskan Fire Emissions Database (AKFED) between 2001 and 2012, and (b) belowground carbon consumption of field data and AKFED. Data is plotted in the middle of interval boundaries on the x axis.

5.2 Environmental variables controlling carbon consumption

5.2.1 Elevation

Elevation was the most important variable in the multiplicative depth of burn model and contributed to the skill of the belowground carbon consumption model (Fig. 4). Barrett et al. (2010, 2011) and Turetsky et al. (2011) demonstrated the explanatory power of topographic variables for belowground carbon consumption in black spruce forests. Kasischke and Hoy (2012) drew upon these findings and assigned seasonal trajectories of carbon consumption to three different topographic classes. The predictive power of elevation for belowground carbon consumption is likely explained by two effects. Elevation captures the spatial distribution of cold temperatures that limit the development of soils and black spruce establishment at the higher elevations (Fig. S7a). Elevation also captures the fuel moisture controls resulting in generally wetter fuels at lower elevations. This moisture control is dynamic through the fire season, and this is captured in our

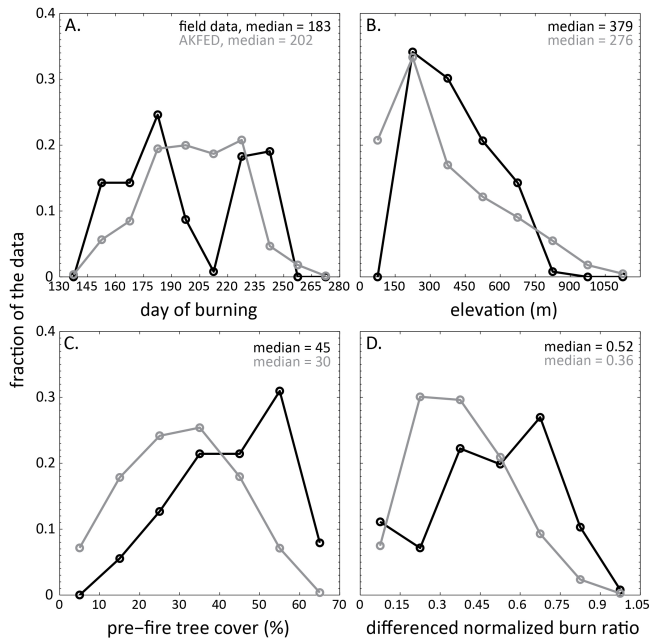


Figure 10. Distribution of (a) day of burning, (b) elevation, (c) pre-fire tree cover, (d) differenced normalized burn ratio of field observations ($n = 126$) and region-wide Alaskan Fire Emissions Database (AKFED) between 2001 and 2012. The tree cover and differenced normalized burn ratio derived from the Moderate Resolution Imaging Spectroradiometer were converted to their Landsat-like values using the equations in Fig. S5. Data is plotted in the middle of interval boundaries on the x axis.

model by interactions between elevation and day of burning (Fig. 4). Inclusion of the northness and slope variables did not improve our model prediction. This contrasts with the findings of Barrett et al. (2010, 2011) who ranked slope and aspect, and derived drainage indicators, in the top predictors for depth of burn. It contrasts with Turetsky et al. (2011) who found differences in average carbon consumption among different aspect classes. As an individual variable, slope did display some explanatory power (Figs. S7b and S8b), but did not contribute to the final model. The contrasting findings of this study compared to Barrett et al. (2010, 2011) and Turetsky et al. (2011) can partly be explained by the scale-dependency of controls on carbon consumption. Here we developed our multiplicative regression model treating all data points within and across different burns with equal weighting. With this assumption, the topographic variable explaining most of the variability in belowground carbon consumption (as a proxy of drainage condition and soil organic layer thickness) was elevation. At a more local scale, for example within one fire, differences in elevation may be smaller, and the variability in drainage conditions and hence belowground carbon consumption may be better captured by including slope and aspect variables. Hollingsworth et al. (2006) found a similar scale-dependency explaining the occurrence and abundance of black spruce types from local to regional scales. Further

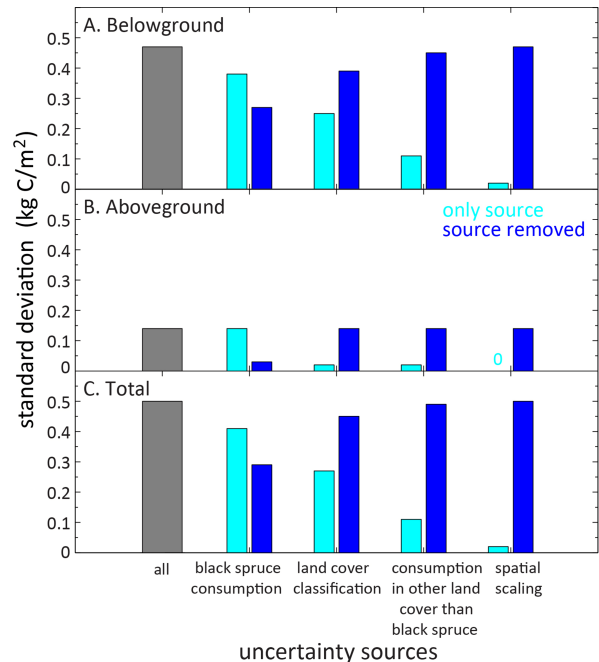


Figure 11. Attribution of uncertainty sources in (a) belowground, (b) aboveground and (c) total carbon consumption estimates. The standard deviation of the consumption estimates from 1000 Monte Carlo simulations was calculated for each scenario.

improvements of the model in future work could include fine-scale drainage effects driven by slope and aspect. More field observations are needed to robustly separate these different topographic effects.

5.2.2 Day of burning

Day of burning within the fire season was the most important variable in the belowground carbon consumption model (Fig. 4). Day of burning is used as a proxy for seasonal drying of the soil organic layer (Turetsky et al., 2011; Kasischke and Hoy, 2012; Genet et al., 2013). This, however, also depends on elevation as lower elevations will thaw and dry earlier than higher elevations. Because of typically drier conditions of the belowground fuel later in the season, late-season fires tend to have higher carbon consumption rates (Figs. 6, 7b, S8d). We found the magnitude of this seasonal change to be smaller than previously reported by Turetsky et al. (2011) and implemented by Kasischke and Hoy (2012). Replacement of day of burning and elevation with weather indices in future work may enable broadening the geographical scope of the current regional carbon consumption model to other regions of boreal North America. This could include components from the Canadian fire-weather index system, (Van Wagner, 1987), such as the drought code, possibly with modifications that account for differences in topographic conditions (Waddington et al., 2012).

5.2.3 Burn severity (dNBR)

The utility of dNBR in the boreal region has been subject to much debate (French et al., 2008). We found a relatively strong relationship between dNBR and aboveground carbon consumption (Fig. S9a). The criticism on the use of dNBR, however, has focused on its ability to predict belowground carbon consumption (French et al., 2008; Hoy et al., 2008). Some authors have found relatively strong correlations between field measures of belowground consumption and dNBR (Hudak et al., 2007; Verbyla and Lord, 2008; Rogers et al., 2014). Barrett et al. (2011) also ranked dNBR in the top third of predictors of a set of 35 spectral and non-spectral environmental variables. French et al. (2008) concluded that the use satellite-based assessments of burn severity, including dNBR, in the boreal region “need to be used judiciously and assessed for appropriateness based on the users’ needs”. We found here that, as an individual variable, dNBR was the top predictor of depth of burn in black spruce forests together with pre-fire tree cover (Fig. S7). We also found that including dNBR in the model resulted in additional explained variance compared to models that excluded dNBR (Fig. 4). In addition, dNBR and tree cover were found to vary at a finer spatial scale than elevation or day of burning (Fig. S12), and their inclusion in the model as such likely improved the representation of the spatial heterogeneity in carbon consumption. Previous work has included variables as fire size and total annual burned area as predictor variables in pyrogenic carbon consumption model (Barrett et al., 2010, 2011; Kasischke and Hoy, 2012; Genet et al., 2013). The significant positive correlations between fire size and mean dNBR (Spearman $r = 0.63$, $p < 0.001$) and annual burned area and mean dNBR (Spearman $r = 0.73$, $p < 0.05$) provided additional support for the inclusion of the dNBR as a synergistic variable in our carbon emissions modeling framework. The advantage of using dNBR for capturing this variability compared to fire size or total annual burned area is that it enables independent assessment of carbon losses at each pixel. It also provides a more mechanistic underpinning for exploring relationships that emerge at the fire-wide or regional level, including the relationships described above between fire size and carbon consumption.

The relatively high correlations between depth of burn, and dNBR and tree cover suggest that crown fires in high density black spruce plots may contribute to deeper burning into the ground layer. Burning into the ground layer is primarily controlled by fuel moisture in the ground layer, which was modeled here as a function of elevation and day of burning. For a given moisture condition of the ground layer, determined by elevation and fire seasonality, dNBR thus adds complementary power for the prediction of the consumption of the ground layer. This may explain why the dNBR has performed well in studies that focused on one single fire in which the elevation and day of burning were relatively constant (Hudak et al., 2007; Verbyla and Lord, 2008; Rogers

et al., 2014). When used over large areas and over a range of burn conditions, our results suggest that the synergistic use of the dNBR with other environmental variables is essential. This finding agrees with Barrett et al. (2010, 2011), who found that a combination of spectral and non-spectral data optimized depth of burn prediction in black spruce forest.

5.2.4 Tree cover

This is the first study to evaluate the potential of tree cover as a predictor of carbon consumption in black spruce forests. The relatively strong relationship between tree cover and aboveground carbon consumption is intuitive as black spruce forest mostly experience stand-replacing crown fires and tree cover is directly related to the amount of available biomass and the probability that the crown fire can spread from tree to tree. Its utility for predicting belowground carbon consumption is less obvious and more indirect. We included tree cover in our analysis since we hypothesized that it would be a good proxy of stand age and site productivity which directly relates to drainage conditions, and thickness and density of the organic layer (Kasischke and Johnstone, 2005; Beck et al., 2011b; Rogers et al., 2013). High intensity crown fires in dense black spruce plots also may provide more radiant heating (and drying) of the ground layer, enabling deeper burns. Significant relationships between tree cover and depth of burn (Fig. S7e), and tree cover and belowground carbon consumption (Fig. S8e) provided support for these mechanisms.

5.3 Comparison with previous work on spatially explicit carbon consumption modeling for boreal fires in Alaska

Here we compare our estimates of carbon emissions and carbon consumption with those from Kasischke and Hoy (2012) and Tan et al. (2007) for the subset of years reported in these publications. For 2004, we estimated a total emission of 69 Tg pyrogenic carbon in our domain. This estimate is slightly higher than the estimate of 65 Tg C from Kasischke and Hoy (2012), and both our estimate and the estimate of Kasischke and Hoy (2012) are substantially lower than the estimate of 81 Tg C reported by Tan et al. (2007). AKFED and Kasischke and Hoy (2012) also yielded similar estimates for the small fire years 2006 and 2008. The two models had diverging predictions for 2007, however, with the domain-wide AKFED estimate of 5 Tg C substantially higher than the estimate of approximately 2 Tg C by Kasischke and Hoy (2012). The discrepancy can be explained in part by the inclusion of the large Anaktuvuk tundra fire within the AKFED domain, whereas the analysis by Kasischke and Hoy (2012) only considered fires in the boreal interior of Alaska.

We also found close agreement in the regional burned area estimates from AKFED and Kasischke and Hoy (2012).

For example for the large fire years of 2004 and 2005, AKFED estimated a burned area of 2295 and 1669 kha, compared to estimates of 2178 and 1492 kha from Kasischke and Hoy (2012). The close agreement between AKFED and the Kasischke and Hoy (2012) for burned area is expected since they use similar input data. Both approaches, for example, use fire perimeter data in combination with spectral screening to estimate burned area.

Carbon consumption estimates for the large fire year 2004 were fairly similar among estimates from Kasischke and Hoy (2012) (3.0 kg C m^{-2}), Tan et al., (2007) (3.1 kg C m^{-2}) and AKFED (3.0 kg C m^{-2}). Both AKFED and Kasischke and Hoy (2012) estimated lower consumption values for the small fire years 2006, 2007 and 2008, although the estimates from Kasischke and Hoy (2012) ($1.5\text{--}1.9 \text{ kg C m}^{-2}$) were lower than AKFED ($1.8\text{--}2.6 \text{ kg C m}^{-2}$). Kasischke and Hoy (2012) used observations derived conceptually from observations reported by Turetsky et al. (2011) that indicated that ground layer consumption increased with fire season progression. We derived a similar relationship with day of burning using a different set of data and statistical approach (Figs. 6 and 7b). We found that, in our application, the non-linear multiplicative regression model outperformed other statistical methods for extrapolating carbon consumption in space and time (Fig. S4). Our depth of burn model achieved a R^2_{adjusted} of 0.40, which is similar to the explained variance of 50 % in estimating relative loss of the organic layer by Genet et al. (2013). An important difference between these estimates is that Genet et al. (2013) aggregated multiple field locations within the same fire by topographic class. We aimed at preserving the within-fire variability by using spatially varying dNBR and tree cover observations as model drivers (Fig. S11). The representation of these higher resolution dynamics in fuel and consumption variability may partly explain our slightly lower model performance.

We further compared AKFED burned area, carbon consumption and emissions estimates with estimates from two larger-scale models, WFEIS and GFED3s. French et al. (2011) compared 11 different estimates of burned area and carbon emissions for the 2004 Boundary fire. Fire-wide burned area estimates ranged between 185 kha and 218 kha, and carbon emissions between 2.8 and 13.3 Tg. The burned area and carbon emissions estimates from AKFED were 205 kha and 6.0 Tg C – similar to the multi-model mean. Our carbon emissions estimate for this fire was slightly higher than estimates from WFEIS (5.3–5.7 Tg C) and field assessment by E. Kasischke (4.8 Tg C) in French et al. (2011). The difference between AKFED and the latter estimate is at least partly explained by differences in burned area, with the field assessment of E. Kasischke in French et al. (2011) reporting a total that was about 10 % lower than AKFED. GFED3 reported 207 ha and 4.64 Tg C emissions for this fire.

Decadal-scale comparison between AKFED, WFEIS and GFED3s demonstrated fairly similar burned area estimates, although AKFED and GFED3s were slightly higher than

WFEIS (Table 2). The similarity between the burned area from AKFED, WFEIS, and GFED3s is not surprising since they operate with similar algorithms. All algorithms look at changes in a spectral index derived from MODIS surface reflectance imagery to map burned area. Burned area in GFED3s and WFEIS were from the MCD64A1 product (Giglio et al., 2009), complemented with small fire contributions outside the MCD64A1 burned area detections for GFED3s (Randerson et al., 2012). AKFED used active fire detections that occurred outside the fire perimeters to include contributions from small fires. The contribution from small fires that were included in GFED3s and AKFED may explain the slightly higher burned area estimates than in WFEIS.

Carbon consumption was not correlated between different models (Table 2). In addition, carbon consumption was slightly lower in GFED3s compared to AKFED, and significantly higher in WFEIS compared to AKFED. This suggests that GFED3s slightly underestimates carbon consumption from boreal fires, although the difference in mean carbon consumption between AKFED and GFED3s is within the range of the region-wide mean uncertainty estimate of 0.50 kg C m^{-2} (Fig. 11). The comparison also indicates that region-wide WFEIS estimates are several fold higher than those from AKFED, GFED3s, or Kasischke and Hoy (2012). The high levels of carbon consumption in WFEIS for Alaska are consistent with the study of Billmire et al. (2014) that showed for the contiguous US WFEIS estimates were about double of GFED3 estimates. Differences in the carbon emissions estimates between approaches result from differences in the methods and input data to quantify burned area, fuel type, and carbon consumption. Billmire et al. (2014) found that the difference between WFEIS and GFED3 carbon emission estimates in the contiguous US was primarily driven by the higher fuel loads assigned in WFEIS. This effect may also explain the discrepancy in Alaska, and further effort is needed to compare the different modeling approaches. These findings also highlight the need for synthesis and inter-comparisons of the different data inputs required for emission modeling, including fuel load, combustion completeness, and emission factors. Such efforts are ongoing (van Leeuwen and van der Werf, 2011; van Leeuwen et al., 2014); van Leeuwen et al. (2013) for example assessed the impact of different sets of emission factors on CO mixing ratios. One constraint with large-scale models is that their coarse spatial resolution does not allow direct comparison with field measurements. This gap may be filled by regional models like AKFED that are calibrated with field data at a higher spatial resolution and can be scaled to a coarser resolution.

5.4 Uncertainties

The domain-wide mean uncertainty for carbon consumption was slightly lower than 20 % of the mean, and similar to fire-wide uncertainty reported by Rogers et al. (2014). Our approach integrated observed and best-guess uncertainty es-

timates for different aspects of our modeling system, including components originating from comparisons of our model with field observations and other components associated with spatial scaling. Other studies reporting region-wide carbon emissions and uncertainties from Alaskan fires have relied on scenarios in which uncertainties of different sources were assigned based on expert knowledge (French et al., 2004; Kasischke and Hoy, 2012). These studies report uncertainty levels in the range of 5–30 %, expressed as the coefficient of variation (standard deviation/mean). For AKFED, the most important source of uncertainty originated from the belowground carbon consumption model for black spruce (Fig. 11). This result is consistent with findings from French et al. (2004) and Kasischke and Hoy (2012) who both identified ground layer consumption as a major source of uncertainty within boreal forest ecosystems.

While we identified and quantified four main sources and their relative importance within AKFED, other sources of uncertainty were not included in our analysis. These include the dNBR threshold used for burned area mapping and other aspects of our burned area algorithm, the assumption of the same controls on pyrogenic carbon consumption in non-black spruce ecosystems, consumption of woody debris, and uncertainties in field measurements. In places where uncertainties in burned area mapping are large, this variable can be the most important source of uncertainty (French et al., 2004; van der Werf et al., 2010; Kasischke and Hoy, 2012). We used three independent data sets (ALFD perimeters, and MODIS surface reflectance and thermal anomalies) to map burned area, including burned area outside ALFD perimeters (1 % of total burned area) and excluding unburned islands within the fire perimeters (18 % of perimeter area). We believe that this approach for mapping burned area was relatively robust and minimized uncertainties from this source.

A more significant uncertainty in estimating region-wide fire emissions comes from a paucity of field observations in ecosystems other than black spruce. Here we assumed that the same environmental variables that controlled carbon consumption in black spruce ecosystems also operated for white spruce and deciduous forest, grassland, and shrub land. This assumption may not entirely be valid but cannot be verified until more field data becomes available for these cover types. Another important source of uncertainty originates from consumption of coarse woody debris. Consumption of coarse woody debris is difficult to quantify and was not explicitly accounted for in our approach. Carbon consumption in this pool is small compared to the consumption of the soil organic layers, but can amount up to 5–7 % of the total consumption (Kasischke and Hoy, 2012). Thus, our model estimates may have a small low bias as a consequence of our lack of explicitly accounting for this pool. Field measurements of fuel loads of woody debris in unburned stands in function of stand age and their combustion in relation to fire-weather conditions may allow for improved models of pyrogenic carbon consumption in boreal forest ecosystems.

Finally, uncertainties within the set of available field data have not been systematically assessed. These may stem from different methods that were used to estimate depth of burn in the field (combustion rods, adventitious roots technique or unburned–burned site pairing) and assumptions used to convert depth of burn measurements to carbon loss (Rogers et al., 2014). For example, the carbon-depth curves used in this study for the Turetsky et al. (2011) data are based on multiple measurements per landscape class and have an inherent uncertainty (Turetsky et al., 2011). In addition, the source and spatial resolution of the DEM may add some additional uncertainty to conversion of the depth of burn observations to belowground carbon consumption for these field plots. While the Rogers et al. (2014) data were collected with the aim of making comparisons with 30 m geospatial layers, some of the other available observations may not have used the same criteria for homogeneity in surrounding areas, and thus may contribute to uncertainties when integrated with other geospatial data.

5.5 Representativeness of the field data

The state-wide median belowground carbon consumption estimate of 2.32 kg C m^{-2} of this study is lower than the median values of the field data used in this study (Fig. 9). The median belowground carbon consumption estimate increased to 2.67 kg C m^{-2} when only pure black spruce stands were considered (Fig. 9b). This value was still considerably lower than the median of 3.10 kg C m^{-2} from the field data used in this study. The field data were, relative to the state-wide distribution, disproportionally sampled in mid-elevation areas with high tree cover and high dNBR (Fig. 10). This suggests that the field measurements of carbon consumption in black spruce forest here were biased towards areas that tend to have higher levels of carbon consumption. Part of this bias may be a consequence of many data being collected from burns during large and severe fire year 2004 (85 out of the 126 plots). We found that large fires years generally have higher carbon consumption estimates (Fig. 8). This corroborates findings of Turetsky et al. (2011) and Kasischke and Hoy (2012), although the relative increase of carbon consumption with higher annual burned area from AKFED was less than reported in these studies. We also found support for the finding of Duffy et al. (2007) and Beck et al. (2011a) that fire size and carbon consumption level are positively correlated.

Several aspects of our analysis call for a more comprehensive field data set to better constrain observation-driven empirical models of pyrogenic carbon consumption in boreal ecosystems. First, additional field efforts could focus on increasing the number of observations in black spruce ecosystems using pre-fire tree cover, post-fire dNBR, topographic conditions, and fire seasonality in the sampling design in an effort to better represent the distribution of burning conditions (Fig. 10). Second, considerable uncertainty within AKFED originated from assumptions made to estimate car-

bon consumption in white spruce, deciduous, grassland, and shrub land ecosystems. Very little data on pyrogenic carbon consumption is currently available for these ecosystems and explicitly targeting these ecosystems is needed to reduce uncertainties in future work. For white spruce and deciduous ecosystems we developed scaling factors using Consume 3.0 (Fig. S6). For grassland and shrub land ecosystems we used the black spruce model because tree cover is one of our predictor variables and our model was calibrated for a range of tree cover between 14 and 64 %. Lower tree cover resulted in lower carbon consumption (Fig. 7e), and this may justify the use of the model for non-treed ecosystems until consumption data within these ecosystems becomes available. Mack et al. (2011) estimated a mean carbon loss of 2.02 kg C m^{-2} with a standard error of 0.44 kg C m^{-2} for the Anaktuvuk River fire. In comparison, our model estimated a mean carbon consumption of 2.56 kg C m^{-2} with a mean pixel-based uncertainty of 0.54 kg C m^{-2} for this event.

Even with an abundance of high quality plot data along key axes of environmental variability, regional extrapolation requires accurate maps of land-cover. To date, the FCCS classification is the only classification that for example distinguishes between black spruce and white spruce in Alaska. No formal accuracy assessment of this layer has been conducted; however, we found that, at its native 30 m resolution, 60 out of the 126 black spruce plots from the field data set (Sect. 2.2) were misclassified; 29 as white spruce, 14 as tundra–grass–shrub, 12 as deciduous, and 5 as non-vegetated. We also found that of eight white spruce–aspen plots from Rogers et al. (2014), seven were classified as black spruce, and one as shrub–grass–tundra. The sample size of the land-cover ground truth data available was too small to robustly quantify potential over- or underrepresentation of land-cover types in the FCCS layer. An improved land-cover characterization, including quantitative uncertainty estimates, is thus essential for reducing region-wide uncertainties. An underrepresentation of the black spruce cover in the FCCS would result in lower state-wide average carbon consumption estimates and vice versa. While some land-cover types, such as spruce and deciduous cover, are likely well separable from remote-sensing based on spectral and phenological characteristics, more detailed distinctions, for example between black and white spruce, may be more challenging but not impossible with the combined use of structural and optical attributes (e.g., Goetz et al., 2010). More than a decade after the call from French et al. (2004) for more field data, including ecosystems that burn less regularly, more field measurements are still required to better constrain pyrogenic carbon consumption in boreal forest ecosystems.

5.6 Future applications

Databases of burned area, severity and emissions with high spatial and temporal resolution like AKFED are a necessity to advance several related fields in biogeosciences. They allow for a more thorough evaluation of models used to relate weather, fuels and topography to fire spread rates that were originally derived using laboratory measurements (Rothermel, 1972; Beer, 1991). Spatially explicit burned area data with high temporal resolution will also allow for quantitative assessments of constraints on fire progression due to fuel discontinuities and fire weather (Krawchuk et al., 2006). Knowledge of these constraints on fire spread may prove valuable when predicting future fire regimes that will result from changes in fire weather, vegetation dynamics, and inherent landscape heterogeneity.

Fire emission databases with high temporal and spatial resolution also may enable improvements in our understanding of fire aerosol composition and decrease the large uncertainties that currently exist in fire emission factors of different gas species by enabling more accurate comparisons with in situ measurements. Fire emissions estimates and atmospheric transport models need to be convolved at high spatial and temporal resolution to capture interactions between emissions, transport, chemical transformation, and deposition of aerosol and trace gas species. In addition, fires in the boreal region are episodic and most of the burned area and emissions occur in a relatively short amount of time. High resolution time series are therefore of paramount importance to infer and forecast possible health effects in populated areas exposed to smoke plumes (Hyer et al., 2007).

6 Conclusions

By integrating field and remote-sensing variables at multiple scales, we developed a database of burned area and carbon emission by fire at 450 m spatial resolution and daily temporal resolution for the state of Alaska between 2001 and 2012. We found that, although most of the fires burned in black spruce forest, considerable burned area in white spruce forest, deciduous forest, and grassland and shrub land ecosystems contributed to lower region-wide carbon consumption estimates. This partly explained why the median carbon consumption of 2.54 kg C m^{-2} over the spatiotemporal domain was lower than that typically observed in black spruce ecosystems. However, even when solely considering pure black spruce pixels, median carbon consumption was still lower than most field observations. This suggests that the available field data that were used in this study may have a bias toward high carbon consumption. We thus recommend caution in extrapolating these values over large areas without taking into account spatial heterogeneity in tree cover and other variables influencing fuels and combustion over the landscape. More comprehensive field databases of car-

bon consumption in black spruce and other ecosystems (e.g., white spruce, deciduous, and tundra ecosystems) are required to better constrain region-wide carbon emissions and lower uncertainties. Further improvements in land-cover characterization are also required to remove potential biases that may originate from uncertainties in this layer.

Our carbon consumption model was driven by four environmental variables: elevation, day of burning, differenced normalized burn ratio (dNBR) and pre-fire tree cover. At the regional level of our study, elevation controlled fuel moisture conditions and soil organic layer thickness. Day of burning within the fire season, in combination with elevation, was used to estimate the seasonal thawing of the active layer and subsequent moisture content of organic soil layers. dNBR and tree cover explained additional model variance, and allowed to capture fine-scale variability in carbon consumption. While the use of dNBR as stand-alone indicator of belowground carbon consumption by fire in boreal ecosystems may have limitations, our model system benefited from its use in synergy with other environmental variables. Higher dNBR values were significantly related to deeper burning in soil organic carbon layers. The observed relationships between belowground carbon consumption, dNBR and tree cover, suggest aboveground fuel consumption and heat release may influence the drying of surface fuels, and vice versa, thus contributing to higher levels of carbon consumption.

The Alaskan Fire Emissions Database (AKFED) is publicly available from sites.google.com/a/uci.edu/sander-veraverbeke/akfed. This data could further contribute to the knowledge on spatiotemporal patterns, controls and limits on fire progression, air pollution and exposure, and aerosol composition of boreal fires.

The Supplement related to this article is available online at doi:10.5194/bg-12-3579-2015-supplement.

Author contributions. S. Veraverbeke designed the study, performed the analyses and wrote the manuscript with inputs from B. M. Rogers and J. T. Randerson at all stages.

Acknowledgements. This work was funded by the National Aeronautics and Space Administration Carbon in Arctic Reservoirs Vulnerability Experiment (CARVE) and NNX11AF96G project. We would like to thank the authors from the Boby et al. (2010) and Turetsky et al. (2011) papers for making their field data publicly available. We are grateful to several colleagues of the University of California, Irvine for discussions on the work. We are thankful to four reviewers, including E. Kasischke and E. Kane, for constructive comments that considerably improved the discussions version of this manuscript.

Edited by: A. Ito

References

- Abatzoglou, J. T. and Kolden, C. A.: Relative importance of weather and climate on wildfire growth in interior Alaska, *Int. J. Wildland Fire*, 20, 479–486, doi:10.1071/WF10046, 2011.
- Allen, J. L. and Sorbel, B.: Assessing the differenced Normalized Burn Ratio's ability to map burn severity in the boreal forest and tundra ecosystems of Alaska's national parks, *Int. J. Wildland Fire*, 17, 463–475, doi:10.1071/WF08034, 2008.
- Amiro, B. D., Todd, J. B., Wotton, B. M., Logan, K. A., Flannigan, M. D., Stocks, B. J., Mason, J. A., Martell, D. L., and Hirsch, K. G.: Direct carbon emissions from Canadian forest fires, 1959–1999, *Can. J. Forest Res.*, 31, 512–525, doi:10.1139/cjfr-31-3-512, 2001.
- Amiro, B. D., Cantin, A., Flannigan, M. D., and de Groot, W. J.: Future emissions from Canadian boreal forest fires, *Can. J. Forest Res.*, 39, 383–395, doi:10.1139/X08-154, 2009.
- Balshi, M. S., McGuire, A. D., Duffy, P., Flannigan, M., Walsh, J., and Melillo, J.: Assessing the response of area burned to changing climate in western boreal North America using a Multivariate Adaptive Regression Splines (MARS) approach, *Glob. Change Biol.*, 15, 578–600, doi:10.1111/j.1365-2486.2008.01679.x, 2009.
- Barrett, K., Kasischke, E. S., McGuire, A. D., Turetsky, M. R., and Kane, E. S.: Modeling fire severity in black spruce stands in the Alaskan boreal forest using spectral and non-spectral geospatial data, *Remote Sens. Environ.*, 114, 1494–1503, doi:10.1016/j.rse.2010.02.001, 2010.
- Barrett, K., McGuire, A. D., Hoy, E. E., and Kasischke, E. S.: Potential shifts in dominant forest cover in interior Alaska driven by variations in fire severity, *Ecol. Appl.*, 21, 2380–2396, 2011.
- Beck, P. S. A., Goetz, S. J., Mack, M. C., Alexander, H. D., Jin, Y., Randerson, J. T., and Lorant, M. M.: The impacts and implications of an intensifying fire regime on Alaskan boreal forest composition and albedo, *Glob. Change Biol.*, 17, 2853–2866, doi:10.1111/j.1365-2486.2011.02412.x, 2011a.
- Beck, P. S. A., Juday, G. P., Alix, C., Barber, V. A., Winslow, S. E., Sousa, E. E., Heiser, P., Herriges, J. D., and Goetz, S. J.: Changes in forest productivity across Alaska consistent with biome shift, *Ecol. Lett.*, 14, 373–9, doi:10.1111/j.1461-0248.2011.01598.x, 2011b.
- Beer, T.: The interaction of wind and fire, *Bound.-Lay. Meteorol.*, 54, 287–308, 1991.
- Billmire, M., French, N. H. F., and Mobley, K.: Comparison of WFEISv0. 3 and GFED3 fire emissions models, available at: http://wfeis.mtri.org/media/Docs/Comparison_of_WFEIS_and_GFED_Fire_Emissions_Models_6-23-2014.pdf, last access: 5 June 2015, 2014.
- Boby, L. A., Schuur, E. A. G., Mack, M. C., Verbyla, D., and Johnstone, J. F.: Quantifying fire severity, carbon, and nitrogen emissions in Alaska's boreal forest, *Ecol. Appl.*, 20, 1633–1647, doi:10.1890/08-2295.1, 2010.
- Bonan, G. B.: Environmental factors and ecological processes controlling vegetation patterns in boreal forests, *Landscape Ecol.*, 3, 111–130, doi:10.1007/BF00131174, 1989.
- Bowman, D. M. J. S., Balch, J. K., Artaxo, P., Bond, W. J., Carlson, J. M., Cochrane, M. A., D'Antonio, C. M., Defries, R. S., Doyle, J. C., Harrison, S. P., Johnston, F. H., Keeley, J. E., Krawchuk, M. A., Kull, C. A., Marston, J. B., Moritz, M. A., Prentice, I. C., Roos, C. I., Scott, A. C., Swetnam, T. W., van der Werf, G. R.,

- and Pyne, S. J.: Fire in the Earth system, *Science*, 324, 481–484, doi:10.1126/science.1163886, 2009.
- Chapin, F. S., Mcguire, A. D., Randerson, J., Pielke, R., Baldocchi, D., Hobbie, S. E., Roulet, N., Eugster, W., Kasischke, E., Rastetter, E. B., Zimov, S. A., and Running, S. W.: Arctic and boreal ecosystems of western North America as components of the climate system, *Glob. Change Biol.*, 6, 211–223, doi:10.1046/j.1365-2486.2000.06022.x, 2000.
- Cocke, A. E., Fulé, P. Z., and Crouse, J. E.: Comparison of burn severity assessments using Differenced Normalized Burn Ratio and ground data, *Int. J. Wildland Fire*, 14, 189–198, doi:10.1071/WF04010, 2005.
- Collins, M., Knutti, R., Arblaster, J., Dufresne, J.-L., Fichetef, T., Friedlingstein, P., Gao, X., Gutowski, W. J., Johns, T., Krinner, G., Shongwe, M., Tebaldi, C., Weaver, A. J., and Wehner, M.: Long-term climate change: projections, commitments and irreversibility, in: *Climate Change 2013: The Physical Science Basis. Contributions of Working group I to the Fifth Assessment Report of the Intergovernmental Panel on Climate Change*, edited by: Stocker, F. T., Qin, D., Plattner, G.-K., Tignor, M., Allen, S. K., Boschung, J., Nauels, A., Xia, Y., Bex, V., and Midgley, P. M., Cambridge University Press, Cambridge, United Kingdom, 1029–1136, 2013.
- Cumming, S.: Forest type and wildfire in the Alberta boreal mixed-wood: what do fires burn?, *Ecol. Appl.*, 11, 97–110, 2001.
- De Groot, W. J., Landry, R., Kurz, W. A., Anderson, K. R., Englefield, P., Fraser, R. H., Hall, R. J., Banfield, E., Raymond, D. A., Decker, V., Lynham, T. J., and Pritchard, J. M.: Estimating direct carbon emissions from Canadian wildland fires, *Int. J. Wildland Fire*, 16, 593–606, doi:10.1071/WF06150, 2007.
- De Groot, W. J., Flannigan, M. D., and Cantin, A. S.: Climate change impacts on future boreal fire regimes, *Forest Ecol. Manag.*, 294, 35–44, doi:10.1016/j.foreco.2012.09.027, 2013.
- De Santis, A. and Chuvieco, E.: Burn severity estimation from remotely sensed data: performance of simulation vs. empirical models, *Remote Sens. Environ.*, 108, 422–435, doi:10.1016/j.rse.2006.11.022, 2007.
- Duffy, P. A., Epting, J., Graham, J. M., Rupp, T. S., and Mcguire, A. D.: Analysis of Alaskan burn severity patterns using remotely sensed data, *Int. J. Wildland Fire*, 16, 277–284, doi:10.1071/WF06034, 2007.
- Eidenshink, J., Schwind, B., Brewer, K., Zhu, Z., Quayle, B., and Howard, S.: A project for monitoring trends in burn severity, *Fire ecology*, 3, 3–21, 2007.
- Epting, J., Verbyla, D., and Sorbel, B.: Evaluation of remotely sensed indices for assessing burn severity in interior Alaska using Landsat TM and ETM+, *Remote Sens. Environ.*, 96, 328–339, doi:10.1016/j.rse.2005.03.002, 2005.
- Flanner, M. G., Zender, C. S., Randerson, J. T., and Rasch, P. J.: Present-day climate forcing and response from black carbon in snow, *J. Geophys. Res.*, 112, D11202, doi:10.1029/2006JD008003, 2007.
- French, N. H. F., Kasischke, E. S., and Williams, D. G.: Variability in the emission of carbon-based trace gases from wildfire in the Alaskan boreal forest, *J. Geophys. Res.*, 108, 8151, doi:10.1029/2001JD000480, 2003.
- French, N. H. F., Goovaerts, P., and Kasischke, E. S.: Uncertainty in estimating carbon emissions from boreal forest fires, *J. Geophys. Res.*, 109, D14S08, doi:10.1029/2003JD003635, 2004.
- French, N. H. F., Kasischke, E. S., Hall, R. J., Murphy, K. A., Verbyla, D. L., Hoy, E. E., and Allen, J. L.: Using Landsat data to assess fire and burn severity in the North American boreal forest region: an overview and summary of results, *Int. J. Wildland Fire*, 17, 443–462, doi:10.1071/WF08007, 2008.
- French, N. H. F., de Groot, W. J., Jenkins, L. K., Rogers, B. M., Alvarado, E., Amiro, B., de Jong, B., Goetz, S., Hoy, E., Hyer, E., Keane, R., Law, B. E., McKenzie, D., McNulty, S. G., Ottmar, R., Pérez-Salcriup, D. R., Randerson, J., Robertson, K. M., and Turetsky, M.: Model comparisons for estimating carbon emissions from North American wildland fire, *J. Geophys. Res.*, 116, G00K05, doi:10.1029/2010JG001469, 2011.
- French, N. H. F., McKenzie, D., Erickson, T., Koziol, B., Billmire, M., Endsley, K. A., Yager Scheinerman, N. K., Jenkins, L., Miller, M. E., Ottmar, R., and Pritchard, S.: Modeling Regional-Scale Wildland Fire Emissions with the Wildland Fire Emissions Information System*, *Earth Interact.*, 18, 1–26, doi:10.1175/EI-D-14-0002.1, 2014.
- Genet, H., Mcguire, A. D., Barrett, K., Breen, A., Euskirchen, E. S., Johnstone, J. F., Kasischke, E. S., Melvin, A. M., Bennett, A., Mack, M. C., Rupp, T. S., Schuur, A. E. G., Turetsky, M. R., and Yuan, F.: Modeling the effects of fire severity and climate warming on active layer thickness and soil carbon storage of black spruce forests across the landscape in interior Alaska, *Environ. Res. Lett.*, 8, 045016, doi:10.1088/1748-9326/8/4/045016, 2013.
- Giglio, L., Descloitres, J., Justice, C. O., and Kaufman, Y. J.: An enhanced contextual fire detection algorithm for MODIS, *Remote Sens. Environ.*, 87, 273–282, doi:10.1016/S0034-4257(03)00184-6, 2003.
- Giglio, L., Csiszar, I., and Justice, C. O.: Global distribution and seasonality of active fires as observed with the terra and aqua Moderate Resolution Imaging Spectroradiometer (MODIS) sensors, *J. Geophys. Res.*, 111, G02016, doi:10.1029/2005JG000142, 2006.
- Giglio, L., Loboda, T., Roy, D. P., Quayle, B., and Justice, C. O.: An active-fire based burned area mapping algorithm for the MODIS sensor, *Remote Sens. Environ.*, 113, 408–420, doi:10.1016/j.rse.2008.10.006, 2009.
- Giglio, L., Randerson, J. T., and van der Werf, G. R.: Analysis of daily, monthly, and annual burned area using the fourth-generation global fire emissions database (GFED4), *J. Geophys. Res.-Biogeo.*, 118, 317–328, doi:10.1002/jgrg.20042, 2013.
- Gillett, N. P., Weaver, A. J., Zwiers, F. W., and Flannigan, M. D.: Detecting the effect of climate change on Canadian forest fires, *Geophys. Res. Lett.*, 31, L18211, doi:10.1029/2004GL020876, 2004.
- Goetz, S. J., Sun, M., Baccini, A., and Beck, P. S. A.: Synergistic use of spaceborne lidar and optical imagery for assessing forest disturbance: an Alaska case study, *J. Geophys. Res.*, 115, G00E07, doi:10.1029/2008JG000898, 2010.
- Hall, R. J., Freeburn, J. T., de Groot, W. J., Pritchard, J. M., Lynham, T. J., and Landry, R.: Remote sensing of burn severity: experience from western Canada boreal fires, *Int. J. Wildland Fire*, 17, 476–489, doi:10.1071/WF08013, 2008.
- Hansen, M. C., DeFries, R. S., Townshend, J. R. G., Carroll, M., Dimiceli, C., and Sohlberg, R. A.: Global Percent Tree Cover at a Spatial Resolution of 500 Meters: first Results of the MODIS Vegetation Continuous Fields Algorithm, *Earth Interact.*, 7, 1–15, 2003.

- Héon, J., Arseneault, D. and Parisien, M.-A.: Resistance of the boreal forest to high burn rates, *P. Natl. Acad. Sci. USA*, 111, 13888–13893, doi:10.1073/pnas.1409316111, 2014.
- Hollingsworth, T. N., Walker, M. D., Chapin III, F. S., and Parsons, A. L.: Scale-dependent environmental controls over species composition in Alaskan black spruce communities, *Can. J. Forest Res.*, 36, 1781–1796, doi:10.1139/x06-061, 2006.
- Hoy, E. E., French, N. H. F., Turetsky, M. R., Trigg, S. N., and Kasischke, E. S.: Evaluating the potential of Landsat TM/ETM+ imagery for assessing fire severity in Alaskan black spruce forests, *Int. J. Wildland Fire*, 17, 500–514, doi:10.1071/WF08107, 2008.
- Hu, F. S., Higuera, P. E., Walsh, J. E., Chapman, W. L., Duffy, P. A., Brubaker, L. B., and Chipman, M. L.: Tundra burning in Alaska: linkages to climatic change and sea ice retreat, *J. Geophys. Res.*, 115, G04002, doi:10.1029/2009JG001270, 2010.
- Hudak, A. T., Morgan, P., Bobbitt, M. J., Smith, A. M. S., Lewis, S. A., Lentile, L. B., Robichaud, P. R., Clark, J. T., and McKinley, R. A.: The relationship of multispectral satellite imagery to immediate fire effects, *Fire Ecol.*, 3, 64–90, 2007.
- Huete, A., Didan, K., Miura, T., Rodriguez, E., Gao, X., and Ferreira, L.: Overview of the radiometric and biophysical performance of the MODIS vegetation indices, *Remote Sens. Environ.*, 83, 195–213, doi:10.1016/S0034-4257(02)00096-2, 2002.
- Hyer, E. J., Kasischke, E. S., and Allen, D. J.: Effects of source temporal resolution on transport simulations of boreal fire emissions, *J. Geophys. Res.*, 112, D01302, doi:10.1029/2006JD007234, 2007.
- Jin, Y., Randerson, J. T., Goetz, S. J., Beck, P. S. A., Loranty, M. M., and Goulden, M. L.: The influence of burn severity on postfire vegetation recovery and albedo change during early succession in North American boreal forests, *J. Geophys. Res.*, 117, G01036, doi:10.1029/2011JG001886, 2012.
- Jin, Y., Randerson, J. T., Faivre, N., Capps, S., Hall, A., and Goulden, M. L.: Contrasting controls on wildland fires in Southern California during periods with and without Santa Ana winds, *J. Geophys. Res.-Biogeo.*, 119, 432–450, doi:10.1002/2013JG002541, 2014.
- Johnstone, J. F. and Kasischke, E. S.: Stand-level effects of soil burn severity on postfire regeneration in a recently burned black spruce forest, *Can. J. Forest Res.*, 35, 2151–2163, doi:10.1139/x05-087, 2005.
- Johnstone, J. F., Hollingsworth, T. N., Chapin, F. S., and Mack, M. C.: Changes in fire regime break the legacy lock on successional trajectories in Alaskan boreal forest, *Glob. Change Biol.*, 16, 1281–1295, doi:10.1111/j.1365-2486.2009.02051.x, 2010.
- Jones, B. M., Kolden, C. A., Jandt, R., Abatzoglou, J. T., Urban, F., and Arp, C. D.: Fire behavior, weather, and burn severity of the 2007 Anaktuvuk River Tundra Fire, North Slope, Alaska, *Arct. Antarct. Alp. Res.*, 41, 309–316, doi:10.1657/1938-4246-41.3.309, 2009.
- Kajii, Y., Kato, S., Streets, D. G., Tsai, N. Y., Shvidenko, A., Nilsson, S., McCallum, I., Minko, N. P., Abushenko, N., Altynsev, D., and Khodzer, T. V.: Boreal forest fires in Siberia in 1998: Estimation of area burned and emissions of pollutants by advanced very high resolution radiometer satellite data, *J. Geophys. Res.*, 107, 4745, doi:10.1029/2001JD001078, 2002.
- Kane, E. S., Valentine, D. W., Schuur, E. A., and Dutta, K.: Soil carbon stabilization along climate and stand productivity gradients in black spruce forests of interior Alaska, *Can. J. Forest Res.*, 35, 2118–2129, doi:10.1139/x05-093, 2005.
- Kane, E. S., Kasischke, E. S., Valentine, D. W., Turetsky, M. R., and McGuire, A. D.: Topographic influences on wildfire consumption of soil organic carbon in interior Alaska: implications for black carbon accumulation, *J. Geophys. Res.*, 112, G03017, doi:10.1029/2007JG000458, 2007.
- Kasischke, E. S. and Bruhwiler, L. P.: Emissions of carbon dioxide, carbon monoxide, and methane from boreal forest fires in 1998, *J. Geophys. Res.*, 108, 8146, doi:10.1029/2001JD000461, 2002.
- Kasischke, E. S. and Hoy, E. E.: Controls on carbon consumption during Alaskan wildland fires, *Glob. Change Biol.*, 18, 685–699, doi:10.1111/j.1365-2486.2011.02573.x, 2012.
- Kasischke, E. S. and Johnstone, J. F.: Variation in postfire organic layer thickness in a black spruce forest complex in interior Alaska and its effects on soil temperature and moisture, *Can. J. Forest Res.*, 35, 2164–2177, doi:10.1139/x05-159, 2005.
- Kasischke, E. S. and Turetsky, M. R.: Recent changes in the fire regime across the North American boreal region – Spatial and temporal patterns of burning across Canada and Alaska, *Geophys. Res. Lett.*, 33, L09703, doi:10.1029/2006GL025677, 2006.
- Kasischke, E. S., French, N. H. F., Bourgeau-Chavez, L. L., and Christensen, N. L.: Estimating release of carbon from 1990 and 1991 forest fires in Alaska, *J. Geophys. Res.*, 100, 2941, doi:10.1029/94JD02957, 1995.
- Kasischke, E. S., Williams, D., and Barry, D.: Analysis of the patterns of large fires in the boreal forest region of Alaska, *Int. J. Wildland Fire*, 11, 131–144, doi:10.1071/WF02023, 2002.
- Kasischke, E. S., Turetsky, M. R., Ottmar, R. D., French, N. H. F., Hoy, E. E., and Kane, E. S.: Evaluation of the composite burn index for assessing fire severity in Alaskan black spruce forests, *Int. J. Wildland Fire*, 17, 515–526, doi:10.1071/WF08002, 2008.
- Kasischke, E. S., Verbyla, D. L., Rupp, T. S., McGuire, A. D., Murphy, K. A., Jandt, R., Barnes, J. L., Hoy, E. E., Duffy, P. A., Calef, M., and Turetsky, M. R.: Alaska's changing fire regime – implications for the vulnerability of its boreal forests, *Can. J. Forest Res.*, 40, 1313–1324, doi:10.1139/X10-098, 2010.
- Kasischke, E. S., Loboda, T., Giglio, L., French, N. H. F., Hoy, E. E., de Jong, B., and Riano, D.: Quantifying burned area for North American forests: implications for direct reduction of carbon stocks, *J. Geophys. Res.*, 116, G04003, doi:10.1029/2011JG001707, 2011.
- Keeley, J. E.: Fire intensity, fire severity and burn severity: a brief review and suggested usage, *Int. J. Wildland Fire*, 18, 116–126, doi:10.1071/WF07049, 2009.
- Kelly, R., Chipman, M. L., Higuera, P. E., Stefanova, I., Brubaker, L. B. and Hu, F. S.: Recent burning of boreal forests exceeds fire regime limits of the past 10,000 years, *P. Natl. Acad. Sci. USA*, 110, 13055–13060, doi:10.1073/pnas.1305069110, 2013.
- Key, C. H. and Benson, N. C.: Landscape assessment: ground measurement of severity; the Composite Burn Index, and remote sensing of severity, the Normalized Burn Index, in: FIREMON: Fire Effects Monitoring and Inventory System, edited by: Lutes, D., Keane, R., Caratti, J., Key, C., Benson, N., Sutherland, S., and Grangi, L., USDA Forest Service, Fort Collins, CO, 1–51, 2006.
- Kolden, C. A. and Rogan, J.: Mapping Wildfire Burn Severity in the Arctic Tundra from Downsampled MODIS Data, *Arct. Antarct. Alp. Res.*, 45, 64–76, doi:10.1657/1938-4246-45.1.64, 2013.

- Kolden, C. A., Lutz, J. A., Key, C. H., Kane, J. T., and van Wagendonk, J. W.: Mapped vs. actual burned area within wildfire perimeters: characterizing the unburned, *Forest Ecol. Manag.*, 286, 38–47, doi:10.1016/j.foreco.2012.08.020, 2012.
- Krawchuk, M. A. and Cumming, S. G.: Effects of biotic feedback and harvest management on boreal forest fire activity under climate change, *Ecol. Appl.*, 21, 122–136, doi:10.1890/09-2004.1, 2011.
- Krawchuk, M. A., Cumming, S. G., Flannigan, M. D., and Wein, R. W.: Biotic and abiotic regulation of lightning fire initiation in the mixedwood boreal forest, *Ecology*, 87, 458–468, doi:10.1890/05-1021, 2006.
- Lapina, K., Honrath, R. E., Owen, R. C., Val Martín, M., Hyer, E. J., and Fialho, P.: Late summer changes in burning conditions in the boreal regions and their implications for NO_x and CO emissions from boreal fires, *J. Geophys. Res.*, 113, D11304, doi:10.1029/2007JD009421, 2008.
- Lecina-Diaz, J., Alvarez, A., and Retana, J.: Extreme fire severity patterns in topographic, convective and wind-driven historical wildfires of Mediterranean pine forests, *PLoS One*, 9, e85127, doi:10.1371/journal.pone.0085127, 2014.
- Lentile, L. B., Holden, Z. A., Smith, A. M. S., Falkowski, M. J., Hudak, A. T., Morgan, P., Lewis, S. A., Gessler, P. E., and Benson, N. C.: Remote sensing techniques to assess active fire characteristics and post-fire effects, *Int. J. Wildland Fire*, 15, 319–345, doi:10.1071/WF05097, 2006.
- López García, M. J. and Caselles, V.: Mapping burns and natural reforestation using thematic Mapper data, *Geocarto International*, 6, 31–37, doi:10.1080/10106049109354290, 1991.
- Mack, M. C., Bret-Harte, M. S., Hollingsworth, T. N., Jandt, R. R., Schuur, E. A. G., Shaver, G. R., and Verbyla, D. L.: Carbon loss from an unprecedented Arctic tundra wildfire, *Nature*, 475, 489–92, doi:10.1038/nature10283, 2011.
- Mann, D. H., Scott Rupp, T., Olson, M. A., and Duffy, P. A.: Is Alaska's Boreal Forest Now Crossing a Major Ecological Threshold?, *Arct. Antarct. Alp. Res.*, 44, 319–331, doi:10.1657/1938-4246-44.3.319, 2012.
- Masuoka, E., Fleig, A., Wolfe, R. E., and Patt, F.: Key characteristics of MODIS data products, *IEEE T. Geosci. Remote*, 36, 1313–1323, doi:10.1109/36.701081, 1998.
- McGuire, A. D., Anderson, L. G., Christensen, T. R., Dallimore, S., Guo, L., Hayes, D. J., Heimann, M., Lorenson, T. D., Macdonald, R. W., and Roulet, N.: Sensitivity of the carbon cycle in the Arctic to climate change, *Ecol. Monogr.*, 79, 523–555, doi:10.1890/08-2025.1, 2009.
- Michalek, J. L., French, N. H. F., Kasischke, E. S., Johnson, R. D., and Colwell, J. E.: Using Landsat TM data to estimate carbon release from burned biomass in an Alaskan spruce forest complex, *Int. J. Remote Sens.*, 21, 323–338, doi:10.1080/014311600210858, 2000.
- Oris, F., Asselin, H., Ali, A. A., Finsinger, W., and Bergeron, Y.: Effect of increased fire activity on global warming in the boreal forest, *Environ. Rev.*, 22, 206–219, doi:10.1139/er-2013-0062, 2014.
- Ottmar, R. D.: Wildland fire emissions, carbon, and climate: Modeling fuel consumption, *Forest Ecol. Manag.*, 317, 41–50, doi:10.1016/j.foreco.2013.06.010, 2014.
- Ottmar, R. D., Prichard, S. J., Vihnanek, R. E., and Sandberg, D. V.: Modification and validation of fuel consumption models for shrub and forested lands in the Southwest, Pacific Northwest, Rockies, Midwest, Southeast and Alaska, Seattle, WA, Project No. 98-1-9-06, 2006.
- Ottmar, R. D., Sandberg, D. V., Riccardi, C. L., and Prichard, S. J.: An overview of the Fuel Characteristic Classification System – quantifying, classifying, and creating fuelbeds for resource planning, *Can. J. For. Res.*, 37, 2383–2393, doi:10.1139/X07-077, 2007.
- Parks, S. A.: Mapping day-of-burning with coarse-resolution satellite fire-detection data, *Int. J. Wildland Fire*, 23, 215–223, doi:10.1071/WF13138, 2014.
- Pimont, F., Dupuy, J.-L., and Linn, R. R.: Coupled slope and wind effects on fire spread with influences of fire size: a numerical study using FIRETEC, *Int. J. Wildland Fire*, 21, 828–842, doi:10.1071/WF11122, 2012.
- Prichard, S. J., Ottmar, R. D., and Anderson, G. K.: *Consume 3.0 user's guide*, Seattle, WA, USA, 2006.
- Randerson, J. T., Liu, H., Flanner, M. G., Chambers, S. D., Jin, Y., Hess, P. G., Pfister, G., Mack, M. C., Treseder, K. K., Welp, L. R., Chapin, F. S., Harden, J. W., Goulden, M. L., Lyons, E., Neff, J. C., Schuur, E. A. G., and Zender, C. S.: The impact of boreal forest fire on climate warming, *Science*, 314, 1130–1132, doi:10.1126/science.1132075, 2006.
- Randerson, J. T., Chen, Y., van der Werf, G. R., Rogers, B. M., and Morton, D. C.: Global burned area and biomass burning emissions from small fires, *J. Geophys. Res.*, 117, G04012, doi:10.1029/2012JG002128, 2012.
- Riccardi, C. L., Ottmar, R. D., Sandberg, D. V., Andreu, A., Elman, E., Kopper, K., and Long, J.: The fuelbed: a key element of the fuel characteristic classification system, *Can. J. Forest Res.*, 37, 2394–2412, doi:10.1139/X07-143, 2007.
- Rogers, B. M., Randerson, J. T., and Bonan, G. B.: High-latitude cooling associated with landscape changes from North American boreal forest fires, *Biogeosciences*, 10, 699–718, doi:10.5194/bg-10-699-2013, 2013.
- Rogers, B. M., Veraverbeke, S., Azzari, G., Czimeczik, C. I., Holden, S. R., Mouteva, G. O., Sedano, F., Treseder, K. K., and Randerson, J. T.: Quantifying fire-wide carbon emissions in interior Alaska using field measurements and Landsat imagery, *J. Geophys. Res.*, 119, 1608–1629, 2014.
- Rogers, B. M., Soja, A. J., Goulden, M. L., and Randerson, J. T.: Influence of tree species on continental differences in boreal fires and climate feedbacks, *Nat. Geosci.*, 8, 228–234, doi:10.1038/ngeo2352, 2015.
- Rothermel, R. C.: A mathematical model for predicting fire spread in wildland fuels, Ogden, UT, Project No. INT-115, 1972.
- Roy, D. P., Ju, J., Kline, K., Scaramuzza, P. L., Kovalsky, V., Hansen, M., Loveland, T. R., Vermote, E., and Zhang, C.: Web-enabled Landsat Data (WELD): Landsat ETM+ composited mosaics of the conterminous United States, *Remote Sens. Environ.*, 114, 35–49, doi:10.1016/j.rse.2009.08.011, 2010.
- Sedano, F. and Randerson, J. T.: Multi-scale influence of vapor pressure deficit on fire ignition and spread in boreal forest ecosystems, *Biogeosciences*, 11, 3739–3755, doi:10.5194/bg-11-3739-2014, 2014.
- Seiler, W. and Crutzen, P. J.: Estimates of gross and net fluxes of carbon between the biosphere and the atmosphere from biomass burning, *Climatic Change*, 2, 207–247, doi:10.1007/BF00137988, 1980.

- Sexton, J. O., Song, X.-P., Feng, M., Noojipady, P., Anand, A., Huang, C., Kim, D.-H., Collins, K. M., Channan, S., DiMiceli, C., and Townshend, J. R.: Global, 30 m resolution continuous fields of tree cover: landsat-based rescaling of MODIS vegetation continuous fields with lidar-based estimates of error, *International Journal of Digital Earth*, 6, 427–448, doi:10.1080/17538947.2013.786146, 2013.
- Soja, A. J., Cofer, W. R., Shugart, H. H., Sukhinin, A. I., Stackhouse Jr., P. W., McRae, D. J., and Conard, S. J.: Estimating fire emissions and disparities in boreal Siberia (1998–2002), *J. Geophys. Res.*, 109, D14S06, doi:10.1029/2004JD004570, 2004.
- Soverel, N. O., Perrakis, D. D. B., and Coops, N. C.: Estimating burn severity from Landsat dNBR and RdNBR indices across western Canada, *Remote Sens. Environ.*, 114, 1896–1909, doi:10.1016/j.rse.2010.03.013, 2010.
- Stehman, S. V. and Selkowitz, D. J.: A spatially stratified, multi-stage cluster sampling design for assessing accuracy of the Alaska (USA) National Land Cover Database (NLCD), *Int. J. Remote Sens.*, 31, 1877–1896, doi:10.1080/01431160902927945, 2010.
- Tachikawa, T., Kabu, M., Iwasaki, A., Gesch, D., Oimoen, M., Zhang, Z., Danielson, J., Krieger, T., Curtis, B., Haase, J., Abrams, M., Crippen, R., and Carabajal, C.: ASTER Global Digital Elevation Model Version 2 – Summary of Validation Results, 2011.
- Tan, Z., Tieszen, L. T., Zhu, Z., Liu, S., and Howard, S. M.: An estimate of carbon emissions from 2004 wildfires across Alaskan Yukon River Basin, *Carbon Balance and Management*, 2, 1–8, 2007.
- Tosca, M. G., Randerson, J. T., and Zender, C. S.: Global impact of smoke aerosols from landscape fires on climate and the Hadley circulation, *Atmos. Chem. Phys.*, 13, 5227–5241, doi:10.5194/acp-13-5227-2013, 2013.
- Turetsky, M. R., Kane, E. S., Harden, J. W., Ottmar, R. D., Manies, K. L., Hoy, E., and Kasischke, E. S.: Recent acceleration of biomass burning and carbon losses in Alaskan forests and peatlands, *Nat. Geosci.*, 4, 27–31, doi:10.1038/ngeo1027, 2011.
- van der Werf, G. R., Randerson, J. T., Giglio, L., Collatz, G. J., Mu, M., Kasibhatla, P. S., Morton, D. C., DeFries, R. S., Jin, Y., and van Leeuwen, T. T.: Global fire emissions and the contribution of deforestation, savanna, forest, agricultural, and peat fires (1997–2009), *Atmos. Chem. Phys.*, 10, 11707–11735, doi:10.5194/acp-10-11707-2010, 2010.
- van Leeuwen, T. T. and van der Werf, G. R.: Spatial and temporal variability in the ratio of trace gases emitted from biomass burning, *Atmos. Chem. Phys.*, 11, 3611–3629, doi:10.5194/acp-11-3611-2011, 2011.
- van Leeuwen, T. T., Peters, W., Krol, M. C., and van der Werf, G. R.: Dynamic biomass burning emission factors and their impact on atmospheric CO mixing ratios, *J. Geophys. Res.-Atmos.*, 118, 6797–6815, doi:10.1002/jgrd.50478, 2013.
- van Leeuwen, T. T., van der Werf, G. R., Hoffmann, A. A., Detmers, R. G., Rucker, G., French, N. H. F., Archibald, S., Carvalho Jr., J. A., Cook, G. D., de Groot, W. J., Hély, C., Kasischke, E. S., Kloster, S., McCarty, J. L., Pettinari, M. L., Savadogo, P., Alvarado, E. C., Boschetti, L., Manuri, S., Meyer, C. P., Siegert, F., Trollope, L. A., and Trollope, W. S. W.: Biomass burning fuel consumption rates: a field measurement database, *Biogeosciences*, 11, 7305–7329, doi:10.5194/bg-11-7305-2014, 2014.
- Van Wagner, C. E.: Development and structure of the Canadian forest Fire Weather Index system, Canadian Forestry Service, Ottawa, 1987.
- van Wagendonk, J. W., Root, R. R., and Key, C. H.: Comparison of AVIRIS and Landsat ETM+ detection capabilities for burn severity, *Remote Sens. Environ.*, 92, 397–408, doi:10.1016/j.rse.2003.12.015, 2004.
- Veraverbeke, S. and Hook, S. J.: Evaluating spectral indices and spectral mixture analysis for assessing fire severity, combustion completeness and carbon emissions, *Int. J. Wildland Fire*, 22, 707–720, doi:10.1071/WF12168, 2013.
- Veraverbeke, S., Lhermitte, S., Verstraeten, W. W., and Goossens, R.: The temporal dimension of differenced Normalized Burn Ratio (dNBR) fire/burn severity studies: the case of the large 2007 Peloponnese wildfires in Greece, *Remote Sens. Environ.*, 114, 2548–2563, doi:10.1016/j.rse.2010.05.029, 2010.
- Veraverbeke, S., Sedano, F., Hook, S. J., Randerson, J. T., Jin, Y., and Rogers, B. M.: Mapping the daily progression of large wildland fires using MODIS active fire data, *Int. J. Wildland Fire*, 23, 655–667, 2014.
- Verbyla, D. and Lord, R.: Estimating post-fire organic soil depth in the Alaskan boreal forest using the Normalized Burn Ratio, *Int. J. Remote Sens.*, 29, 3845–3853, doi:10.1080/01431160701802497, 2008.
- Viereck, L. A.: Wildfire in the Taiga of Alaska, *Quaternary Res.*, 3, 465–495, 1973.
- Waddington, J. M., Thompson, D. K., Wotton, M., Quinton, W. L., Flannigan, M. D., Benscoter, B. W., Baisley, S. A., and Turetsky, M. R.: Examining the utility of the Canadian Forest Fire Weather Index System in boreal peatlands, *Can. J. Forest Res.*, 42, 47–58, doi:10.1139/x11-162, 2012.
- Yao, J. and Henderson, S. B.: An empirical model to estimate daily forest fire smoke exposure over a large geographic area using air quality, meteorological, and remote sensing data, *J. Expo. Sci. Env. Epid.*, 24, 328–235, doi:10.1038/jes.2013.87, 2014.
- Yokelson, R. J., Burling, I. R., Gilman, J. B., Warneke, C., Stockwell, C. E., de Gouw, J., Akagi, S. K., Urbanski, S. P., Veres, P., Roberts, J. M., Kuster, W. C., Reardon, J., Griffith, D. W. T., Johnson, T. J., Hosseini, S., Miller, J. W., Cocker III, D. R., Jung, H., and Weise, D. R.: Coupling field and laboratory measurements to estimate the emission factors of identified and unidentified trace gases for prescribed fires, *Atmos. Chem. Phys.*, 13, 89–116, doi:10.5194/acp-13-89-2013, 2013.
- Yuan, F.-M., Yi, S.-H., McGuire, A. D., Johnson, K. D., Liang, J., Harden, J. W., Kasischke, E. S. and Kurz, W. A.: Assessment of boreal forest historical C dynamics in the Yukon River Basin: relative roles of warming and fire regime change, *Ecol. Appl.*, 22, 2091–2109, 2012.